

RESEARCH

Open Access



Extensive identification and analysis of conserved small ORFs in animals

Sebastian D. Mackowiak¹, Henrik Zauber¹, Chris Bielow^{1,2}, Denise Thiel¹, Kamila Kutz¹, Lorenzo Calviello¹, Guido Mastrobuoni¹, Nikolaus Rajewsky¹, Stefan Kempa¹, Matthias Selbach¹ and Benedikt Obermayer^{1*}

Abstract

Background: There is increasing evidence that transcripts or transcript regions annotated as non-coding can harbor functional short open reading frames (sORFs). Loss-of-function experiments have identified essential developmental or physiological roles for a few of the encoded peptides (micropeptides), but genome-wide experimental or computational identification of functional sORFs remains challenging.

Results: Here, we expand our previously developed method and present results of an integrated computational pipeline for the identification of conserved sORFs in human, mouse, zebrafish, fruit fly, and the nematode *C. elegans*. Isolating specific conservation signatures indicative of purifying selection on amino acid (rather than nucleotide) sequence, we identify about 2,000 novel small ORFs located in the untranslated regions of canonical mRNAs or on transcripts annotated as non-coding. Predicted sORFs show stronger conservation signatures than those identified in previous studies and are sometimes conserved over large evolutionary distances. The encoded peptides have little homology to known proteins and are enriched in disordered regions and short linear interaction motifs. Published ribosome profiling data indicate translation of more than 100 novel sORFs, and mass spectrometry data provide evidence for more than 70 novel candidates.

Conclusions: Taken together, we identify hundreds of previously unknown conserved sORFs in major model organisms. Our computational analyses and integration with experimental data show that these sORFs are expressed, often translated, and sometimes widely conserved, in some cases even between vertebrates and invertebrates. We thus provide an integrated resource of putatively functional micropeptides for functional validation *in vivo*.

Background

Ongoing efforts to comprehensively annotate the genomes of humans and other species revealed that a much larger fraction of the genome is transcribed than initially appreciated [1]. Pervasive transcription produces a number of novel classes of non-coding RNAs, in particular long intergenic non-coding RNAs (lincRNAs) [2]. The defining feature of lincRNAs is the lack of canonical open reading frames (ORFs), classified mainly by length, nucleotide sequence statistics, conservation signatures, and similarity to known protein domains [2]. Although coding-independent RNA-level functions have been established for a growing number of lincRNAs [3, 4],

there is little consensus about their general roles [5]. Moreover, the distinction between lincRNAs and mRNAs is not always clear-cut [6], since many lincRNAs have short ORFs, which easily occur by chance in any stretch of nucleotide sequence. However, recent observations suggest that lincRNAs and other non-coding regions are often associated with ribosomes and sometimes in fact translated [7–16]. Indeed, some of the encoded peptides have been detected via mass spectrometry [10, 17–23]. Small peptides have been marked as essential cellular components in bacteria [24] and yeast [25]. More detailed functional studies have identified the well-known *tarsal-less* peptides in insects [26–29], characterized a short secreted peptide as an important developmental signal in vertebrates [30], and established a fundamental link between different animal micropeptides and cellular calcium uptake [31, 32].

* Correspondence: benedikt.obermayer@mdc-berlin.de

¹Berlin Institute for Medical Systems Biology, Max-Delbrück-Center for Molecular Medicine, Robert-Rössle-Str. 10, 13125 Berlin, Germany
Full list of author information is available at the end of the article

Importantly, some ambiguity between coding and non-coding regions has been observed even on canonical mRNAs [15]: upstream ORFs (uORFs) in 5' untranslated regions (5'UTRs) are frequent, well-known, and commonly associated with the translational regulation of the main CDS [33, 34]. To a lesser extent, mRNA 3'UTRs have also been found associated to ribosomes, which has been attributed to stop-codon read-through [35], in other cases to delayed drop-off, translational regulation, or ribosome recycling [36], and even to the translation of 3'UTR ORFs (dORFs) [10]. Translational regulation could be the main role of these ORFs, and regulatory effects of translation (for example, on mRNA stability) could be a major function of lincRNA translation [12]. Alternatively, they could be ORFs in their own right, considering well-known examples of polycistronic transcripts in animals such as the *tarsal-less* mRNA [26–28]. Indeed, many non-annotated ORFs have been found to produce detectable peptides [10, 17], and might therefore encode functional micropeptides [37].

Typically, lincRNAs are poorly conserved on the nucleotide level, and it is hard to computationally detect functional conservation despite sequence divergence even when it is suggested by synteny [2, 38, 39]. In contrast, many of the sORFs known to produce functional micropeptides display striking sequence conservation [26–28, 30, 31], highlighted by a characteristic depletion of non-synonymous compared to synonymous mutations. This suggests purifying selection on the level of encoded peptide (rather than DNA or RNA) sequence. Also, the sequence conservation rarely extends far beyond the ORF itself, and an absence of insertions or deletions implies conservation of the reading frame. These features are well-known characteristics of canonical protein-coding genes and have in fact been used for many years in comparative genomics [40, 41]. While many powerful computational methods to identify protein-coding regions are based on sequence statistics and suffer high false-positive rates for very short ORFs [42, 43], comparative genomics methods have gained statistical power over the last years given the vastly increased number of sequenced animal genomes.

Here, we present results of an integrated computational pipeline to identify conserved sORFs using comparative genomics. We greatly extended our previously published approach [10] and applied it to entire transcriptomes of five animal species: human (*H. sapiens*), mouse (*M. musculus*), zebrafish (*D. rerio*), fruit fly (*D. melanogaster*), and the nematode *C. elegans*. Applying rigorous filtering criteria, we find a total of about 2,000 novel conserved sORFs in lincRNAs as well as other regions of the transcriptome annotated as non-coding. By means of comparative and population genomics, we detect purifying selection on the encoded peptide sequence, suggesting

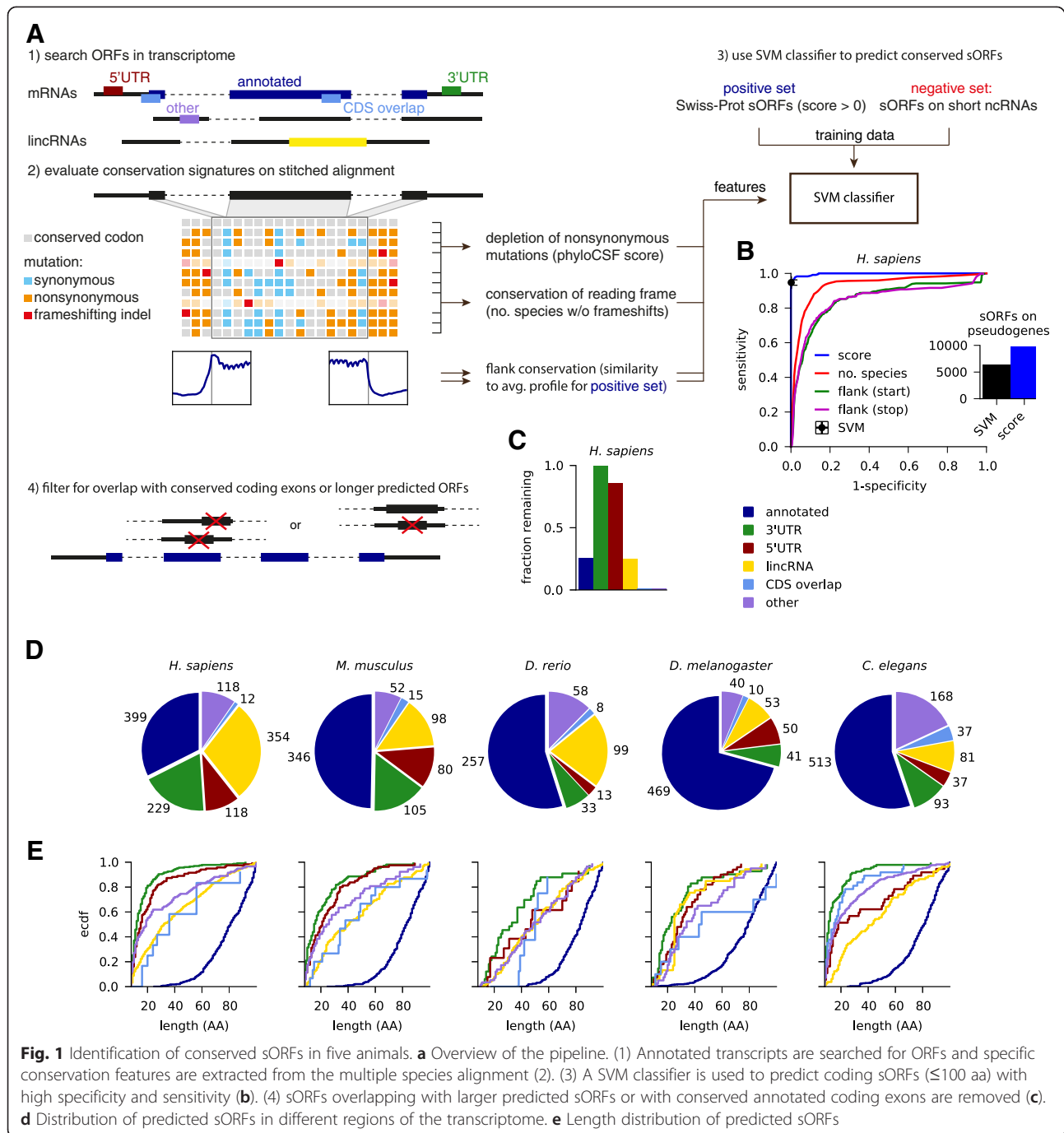
that the predicted sORFs, of which some are conserved over wide evolutionary distances, give rise to functional micropeptides. We compare our results to published catalogs of peptides from non-annotated regions, to sets of sORFs found to be translated using ribosome profiling, and to a number of computational sORF predictions. While there is often little overlap, we find in all cases consistently stronger conservation for our candidates, confirming the high stringency of our selection criteria. Overall, predicted peptides have little homology to known proteins and are rich in disordered regions and peptide binding motifs which could mediate protein-protein interactions. Finally, we use published high-throughput datasets to analyze expression of their host transcripts, confirm translation of more than 100 novel sORFs using published ribosome profiling data, and mine in-house and published mass spectrometry datasets to support protein expression from more than 70 novel sORFs. Altogether, we provide an integrated catalog of conserved sORFs in animals to aid functional studies.

Results

Identification of conserved coding sORFs from multiple species alignments

Our approach, which is summarized in Fig. 1a, is a significant extension of our previously published method [10]. Like most other computational studies, we take an annotated transcriptome together with published lincRNA catalogs as a starting point. We chose the Ensembl annotation (v74), which is currently one of the most comprehensive ones, especially for the species considered here. In contrast to *de novo* genome-wide predictions [44, 45], we rely on annotated transcript structures including splice sites. We then identified canonical ORFs for each transcript, using the most upstream AUG for each stop codon; although use of non-canonical start codons has been frequently described [15–17, 46, 47], there is currently no clear consensus how alternative translation start sites are selected. Next, ORFs were classified according to their location on lincRNAs or on transcripts from protein-coding loci: annotated ORFs serving as positive control; ORFs in 3'UTRs, 5'UTRs or overlapping with the annotated CDS; or on other transcripts from a protein-coding locus lacking the annotated CDS. We ignored pseudogene loci: although pseudogenes have been associated with a variety of biological functions [48–50], their evolutionary history makes it unlikely that they harbor sORFs as independent functional units encoding micropeptides.

Based on whole-genome multiple species alignments, we performed a conservation analysis to obtain four characteristic features for each ORF: most importantly, we scored the depletion of non-synonymous mutations in the alignment using phyloCSF [51]; we also evaluated



conservation of the reading frame from the number of species in the (un-stitched) alignment that lack frameshifting indels; finally, we analyzed the characteristic steps in nucleotide-level conservation (using phastCons) around the start and stop codons by comparing to the mean profile observed in annotated ORFs. Next, we trained a classifier based on support vector machines on confident sets of conserved small peptides and control sORFs from non-coding regions (see Ré *et al.* [52] and Crappé *et al.* [45] for related approaches). As positive

control, we chose conserved small peptides of at most 100 aa from Swiss-Prot with positive phyloCSF score. Here, we discarded a number of presumably fast-evolving peptides: 177 in human and 72 in mouse, which are associated with antimicrobial defense, and 15 in fly of which 11 are signal peptides. As negative control, we chose sORFs on classical ncRNAs such as pre-miRNAs, rRNAs, tRNAs, snRNAs, or snoRNAs. Importantly, both of these sets overlap with a sizable number of genomic regions that are highly conserved on the nucleotide level (phastCons

conserved elements; Additional file 1: Figure S1A). While each of the four conservation features performs well in discriminating positive and negative set (Additional file 1: Figure S1B), their combination in the SVM reaches very high sensitivity (between 1-5 % false negative rate) and specificity (0.1-0.5 % false positive rate) when cross-validating our training data (Fig. 1b and Additional file 1: Figure S1B). The classifier is dominated by the phyloCSF score (Additional file 1: Figure S1B), which is therefore the primarily relevant feature for ranking candidates by confidence. However, the additional conservation features help to reject sORFs on annotated pseudogene transcripts, which typically do not show characteristic steps in nucleotide conservation near start or stop codons (Fig. 1b inset).

We noted that known small proteins typically reside in distinct genomic loci, while many predicted ORFs on different transcript isoforms overlap with one another or with annotated coding exons. Therefore, we aimed to remove candidates where the conservation signal could not be unambiguously assigned. We thus implemented a conservative overlap filter by excluding ORFs overlapping with conserved coding exons or with longer SVM-predicted ORFs (Materials and methods). Most sORFs in 3'UTRs or 5'UTRs pass this filter, but many sORFs from different mRNA and lincRNA isoforms are collapsed, and most sORFs (85-99 %) overlapping with annotated coding sequence are rejected (Fig. 1c and Additional file 1: Figure S1D).

Hundreds of novel conserved sORFs, typically much smaller than known small proteins

With our stringent conservation and overlap filters, we predict 2,002 novel conserved sORFs of nine to 101 codons: 831 in *H. sapiens*, 350 in *M. musculus*, 211 in *D. rerio*, 194 in *D. melanogaster*, and 416 in *C. elegans*. Novel sORFs reside in lincRNAs and transcriptomic regions annotated as non-coding, with relatively few sORFs predicted in 3'UTRs or overlapping coding sequence relative to the size of these transcriptome regions (pre-overlap filter; see Additional file 1: Figure S1C). Our pipeline recovers known or recently discovered functional small peptides, such as all *tarsal-less* peptides [26–28], sarcolamban [32] and *pgc* [53] in flies, *toddler* [30] in zebrafish together with its human and mouse orthologs, and BRK1 [54] and myoregulin [31] in human. We also predict that many transcripts annotated as lincRNAs in fact code for proteins. While it is a relatively small fraction (1-7 %) that includes transcripts in intermediate categories, such as TUCPs in human [55] and RITs in *C. elegans* [56], the percentage increases when looking at conserved lincRNAs: for instance, eight of 29 zebrafish lincRNAs conserved in vertebrates [38] are predicted to contain conserved ORFs, three of which have

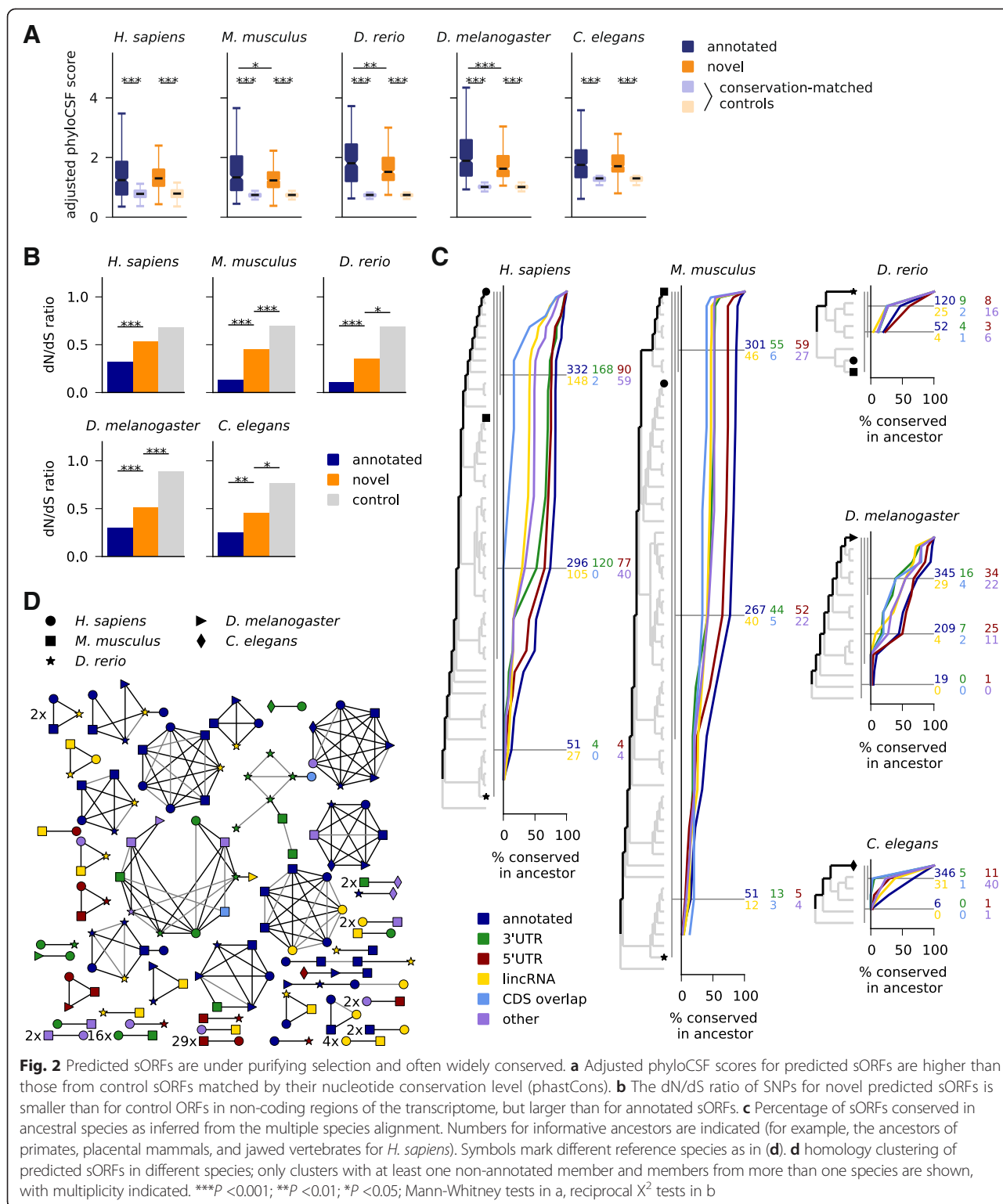
been included in the most recent Ensembl release (v79). Further, we note that a sizable number of uORFs likely encode functional peptides, including the known case of MKKS [57]. Finally, we observe that the great majority of predicted sORFs is much smaller (median length 11 aa for 3'UTR sORFs in *C. elegans* to 49 aa for lincRNA sORFs in *D. rerio*) than annotated sORFs (median length 81-83 aa), with sORFs in 3'UTRs and 5'UTRs typically being among the shortest. In almost all cases, these very short ORFs also span only one exon, while longer sORFs sometimes contain introns (Additional file 1: Figure S1E).

We assembled relevant information for the identified sORFs including coordinates, sequences, transcript models, and features analyzed in the following sections in Additional file 2: Table S1, Additional file 3: Table S2, Additional file 4: Table S3, Additional file 5: Table S4, Additional file 6: Table S5.

Novel sORFs are under purifying selection on the amino acid level

Since selection on the level of the encoded amino acid sequence permits synonymous sequence variation, we compared length-adjusted phyloCSF scores of predicted sORFs to those of control ORFs matched for their nucleotide-level conservation (Fig. 2a, Additional file 7: Figure S2; Materials and methods). As expected from the design of our pipeline, we find that novel predicted sORFs are specifically depleted of non-synonymous mutations, and in most cases to a similar extent as annotated ones. We also collected polymorphism data to perform a similar but independent test on a population genomics level: aggregating SNPs from all predicted sORFs (novel or annotated), we measured the dN/dS ratio and found that non-synonymous SNPs are suppressed compared to synonymous ones to a greater extent than in control regions (Fig. 2b; Materials and methods). Possibly due to a higher number of false positives in the set of novel sORFs, the depletion is less pronounced than for annotated small proteins, and the associated *P* values are lower in the species with higher SNP density (mouse and fruit fly with 16 and 45 SNPs/kb in the control regions) than in zebrafish or *C. elegans* with 1.7 and 2.0 SNPs/kb, respectively. It fails to pass the significance threshold in human with 2.4 SNPs/kb, where we get *P* = 0.076 as the larger value from reciprocal χ^2 tests.

These results confirm that predicted sORFs permit synonymous more than non-synonymous sequence variation when comparing within or between species, indicating that selection acts on the level of the encoded peptide sequence and therefore suggesting functional peptide products.



Some novel sORFs are widely conserved

We next sought to evaluate how widely the predicted sORFs are conserved. First, we took an alignment-based approach: we inferred most recent common ancestors from the alignment by tallying the species with conserved

start and stop codons and (if applicable) splice sites, and without nonsense mutations. This analysis depends on the accuracy of the alignment, but it does not require transcript annotation in the aligned species. Using this method (Fig. 2c) we find that after annotated small proteins,

uORFs are most widely conserved, followed by the other sORF types. Of the novel sORFs found in human, 342 are conserved in placental mammals and 39 in the gnathostome ancestor (that is, in jawed vertebrates). Among sORFs predicted in zebrafish, 18 are conserved in teleosts, 49 fruit fly sORFs are conserved in Drosophilids, and 88 *C. elegans* sORFs are conserved in worms of the *Elegans* group.

We also addressed this question with a complementary analysis: we performed a clustering of sORFs predicted in the different species using a BLAST-based approach adapted for short amino acid sequences (Materials and methods). This analysis clusters 1,445 of in total 3,986 sORFs into 413 similarity groups, and 304 of 2,002 novel predictions are grouped into 138 clusters. The clusters containing at least one novel candidate and sORFs from more than one species are summararily shown in Fig. 2d. We find that 65 of 89 clusters involving novel vertebrate candidates are also supported by synteny (Materials and methods), and that some novel predictions cluster together with sORFs annotated in other species, confirming the reliability of our approach and extending current transcriptome annotations. For instance, several zebrafish lincRNAs are found to encode known small proteins such as cortexin 2, nuclear protein transcriptional regular 1 (NUPR1), small VCP/p97-interacting protein (SVIP), or centromere protein W. Conversely, some lincRNAs from mouse and human encode small peptides with annotated (yet often uncharacterized) homologs in other species. Further, a sORF in the 5'UTR of the worm gene *mnat-1* encodes a peptide with homology to murine *lyrm4* and the fly gene *bcn92*.

We also find 109 clusters of entirely novel predictions, such as 29 sORFs in 5'UTRs and 16 in 3'UTRs conserved between human and mouse, a 15 aa uORF in solute carrier family 6 member 8 (SLC6A8) conserved across vertebrates, or another 15 aa peptide from the 5'UTR of the human gene FAM13B conserved in the 5'UTRs of its vertebrate and fly homologs. One novel 25 aa peptide from annotated lincRNAs is predicted in three vertebrates and four other ones in two out of three. The other 22 human lincRNA sORFs found to be conserved in vertebrates (Fig. 2c) cluster together with annotated sORFs or are not detected in the other species for various reasons: they do not pass the overlap filter, do not use the most upstream start codon, or lack transcript annotation in mouse and zebrafish. Further, besides the 15 aa uORF peptide in FAM13B, there are also several peptides encoded in 3'UTRs or of mixed annotation conserved between vertebrates and invertebrates. Two clusters of unclear significance, consisting mainly of sORFs in the 3'UTRs of zinc-finger proteins, share a common HTGEK peptide motif, a known conserved linker sequence in C2H2 zinc fingers [58]. Finally, we note that our sequence-based approaches

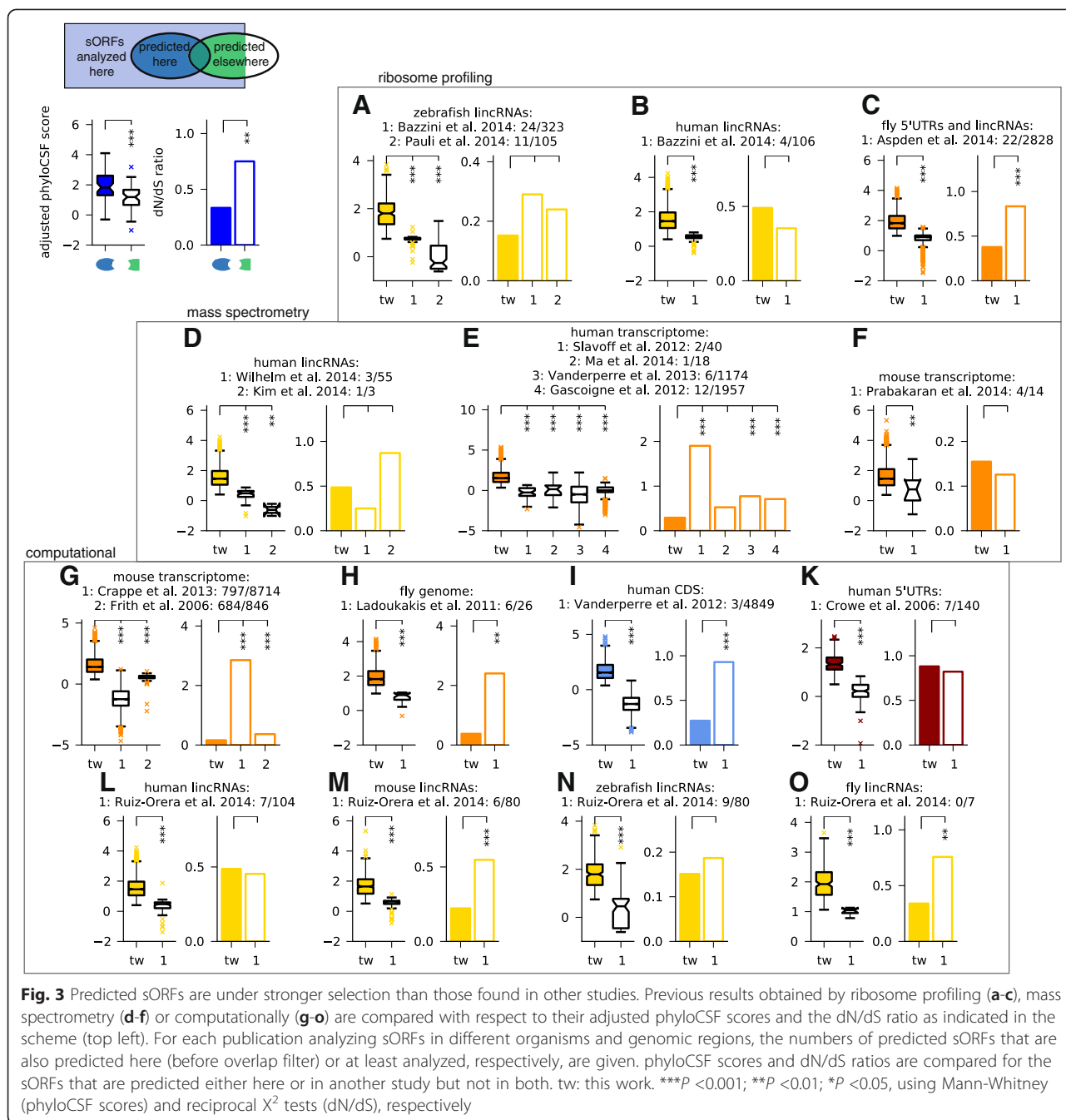
cannot resolve structural and/or functional homologies that persist despite substantial sequence divergence as observed between different animal peptides interacting with the Ca²⁺ ATPase SERCA [31, 32], or between bacterial homologs of the *E. coli* CydX protein [59]. We expect that such homologies between the predicted sORFs could be uncovered using more specialized approaches.

Taken together, this conservation analysis shows that novel sORFs are often widely conserved on the sequence level; further functional homologies could exist that are not detectable by sequence [31, 32].

Conserved sORFs are predicted with high stringency

Many recent studies have addressed the challenge of identifying novel small protein-coding genes by means of computational methods or high-throughput experiments. These studies were performed in different species with different genome annotations, searching in different genomic regions, allowing different length ranges and using often quite different underlying hypotheses, for instance with respect to non-canonical start codons. Accordingly, they arrive at very different numbers. To reconcile these different approaches, we inclusively mapped sORFs defined in 16 other studies with published lists of coordinates, sequences, or peptide fragments, to the comprehensive set of transcriptomic ORFs analyzed here (Additional file 8: Table S6). With the caveat that other studies often prioritized findings by different criteria, we then compared results with regard to the aspect of main interest here: conservation of the encoded peptide sequence, by means of comparative and population genomics as in Fig. 2a and b. We grouped studies by methodology, and by organism and genomic regions analyzed. We then compared sORFs predicted in our study but not in others to sORFs that were predicted elsewhere and analyzed but rejected here (Fig. 3). We used our results before applying the overlap filter. Considering changes in annotation (for example, of coding sequences, lincRNAs and pseudogenes), we only compared to those sORFs that we analyzed and classified into the corresponding category. Generally, we find rather limited overlap between our predictions and results from other studies, which is only partially explained by differences in applied technique and underlying hypothesis (Additional file 9: Figure S3). We also find that the sORFs that we predict for the first time have consistently much higher length-adjusted phyloCSF scores than those found in other studies but rejected in ours; in many cases, we also find that the dN/dS ratio of non-synonymous vs. synonymous SNP density is lower, albeit in a similar number of cases there is not enough data to render the *P* value significant (we used the larger one from reciprocal X²-tests).

First, we compared to several studies using ribosome profiling [10, 11, 30] (Fig. 3a-c): in zebrafish, we obtain similar overlap as reported in our previous publication



[10], the results of which are re-analyzed with the updated transcriptome annotation for comparison. Ribosome profiling provides evidence of translation in the cell types or developmental stages analyzed, but in addition to coding sORFs it also detects sORFs with mainly regulatory functions such as uORFs. Next, we compared to seven studies employing mass spectrometry [17–23]: matching given protein sequences or re-mapping detected peptides to the set of sORFs analyzed here, we find only between one and 12 common results from between three and almost 2,000 sORFs (Fig. 3d-f).

Note that up to 62 % of peptides identified in these studies come from pseudogene loci which we excluded. While mass spectrometry provides direct evidence for peptide products, it is also performed in specific cell lines or tissues and has limited dynamic range. This can prevent detection of small peptides, which might be of low abundance or half-life, or get lost during sample preparation. Both experimental methods cannot distinguish sORFs coding for conserved micropeptides from those coding for lineage-specific or fast-evolving functional products. It is thus not surprising that these

sORFs are as a group less conserved than the ones found using conservation as a selection criterion.

Next, we compared our results against other computational studies [44, 45, 60–63]. Here, we can often match much larger numbers of sORFs, but except for predictions of the CRITICA pipeline in mouse, which uses conservation as well as sequence statistics [60] and favors longer ORFs, we again find only limited overlap: we predict between 0 and 23 % of analyzed sORFs found elsewhere, indicating a high variability in different computational methods, even though many of them use evolutionary conservation as a filter. The consistently better conservation indicators for our results (Fig. 3g-o) confirm that the deeper alignments and sensitive conservation features used here lead to increased performance. However, we remark that our method is not designed to find sORFs in alternative reading frames [63, 64] unless their evolutionary signal strongly exceeds what comes from the main CDS (for example, because it is incorrectly annotated); also, the limited overlap with Ruiz-Orera *et al.* [62] is not unexpected since their focus was on newly evolved lincRNA sORFs, which are by definition not well conserved, but are often translated (Additional file 9: Figure S3). Finally, Crappé *et al.* [45] and Ladoukakis *et al.* [44] limited their search to single-exon sORFs, whereas 66 % and 20 % of sORFs predicted by us in the transcriptomes of mouse and fly, respectively, span more than one exon (Additional file 1: Figure S1E). However, even when restricting the comparison to single-exon sORFs, we find better conservation indicators for our results.

Given the consistently higher phyloCSF scores and often better dN/dS ratios of our sORFs when comparing to other studies, we conclude that our results present a high-stringency set of conserved sORFs coding for putatively functional micropeptides.

Novel peptides are often disordered and enriched for linear peptide motifs

We next investigated similarities and differences of sORF-encoded peptides to annotated proteins. First, we used amino acid and codon usage to cluster predicted sORFs, short and long annotated proteins, and a negative control consisting of ORFs in non-coding transcriptome regions with small phyloCSF scores (Additional file 10: Figure S4). Looking at amino acid usage, we were surprised to find that our novel predictions in four out of five species clustered with the negative control. However, when choosing subsamples of the data, novel predictions also often clustered together with annotated proteins, suggesting that their overall amino acid usage is intermediate, as observed in a related context [65]. Indeed, the frequencies of most amino acids lie between those of positive and negative control. Interestingly, however, we found that novel predictions clustered robustly with annotated

proteins when analyzing codon usage (with the exception of fruit fly).

Dissimilarity with annotated proteins was also confirmed when testing for similarity to the known proteome using BLAST. Only a small fraction of novel predictions, mainly those in the ‘CDS overlap’ and ‘other’ categories, give significant hits (Fig. 4a). While some novel sORFs are homologous to annotated small proteins as revealed by the clustering analysis in Fig. 2c, there is no significant overlap between the sORFs assigned to similarity clusters and those with similarity to known proteins (Fisher’s $P > 0.1$ for all species except for *C. elegans* where $P = 0.003$). Hence, even completely novel sORFs are sometimes conserved over wide distances.

We then hypothesized that differences in amino acid composition might give rise to different structural properties. We used IUPred [66] to detect intrinsically unstructured regions, and found that novel predictions are much more disordered than known small proteins or a length-matched negative control (Fig. 4b). This could suggest that the peptides encoded by conserved sORFs adopt more stable structures only upon binding to other proteins, or else mediate protein-protein or protein-nucleic acid interactions [67]. It has recently become clear that linear peptide motifs, which are often found in disordered regions, can be important regulators of protein function and protein-protein interactions [68]. Indeed, when searching the disordered parts of sORF-encoded peptides for matches to motifs from the ELM database [69], we find that the increased disorder comes with a higher density of such motifs in the predicted peptides (Fig. 4c), as was also observed recently for peptides identified with mass spectrometry [23].

Since a recent study identified *toddler* and a number of other non-annotated ORFs with predicted signal sequences [30], we searched our novel candidates with signalp [70]. Figure 4d shows that a small number of our predicted sORFs contain signal sequences, but this does not exceed expectations from searching a length-matched control set. However, the typically lower amino acid conservation at the N-terminus of signal peptides [30] could imply that some genuine candidates escape our conservation filters.

Taken together, these results show that novel sORF-encoded peptides are different from annotated proteins in terms of amino acid usage and sequence homology, that they are enriched in disordered regions and peptide motifs, and that only few of them contain signal peptides.

3'UTR sORFs are not consistently explained by stop-codon readthrough or alternative terminal exons

sORFs in 3'UTRs (dORFs) are least likely to be predicted as conserved compared to the other categories (Additional

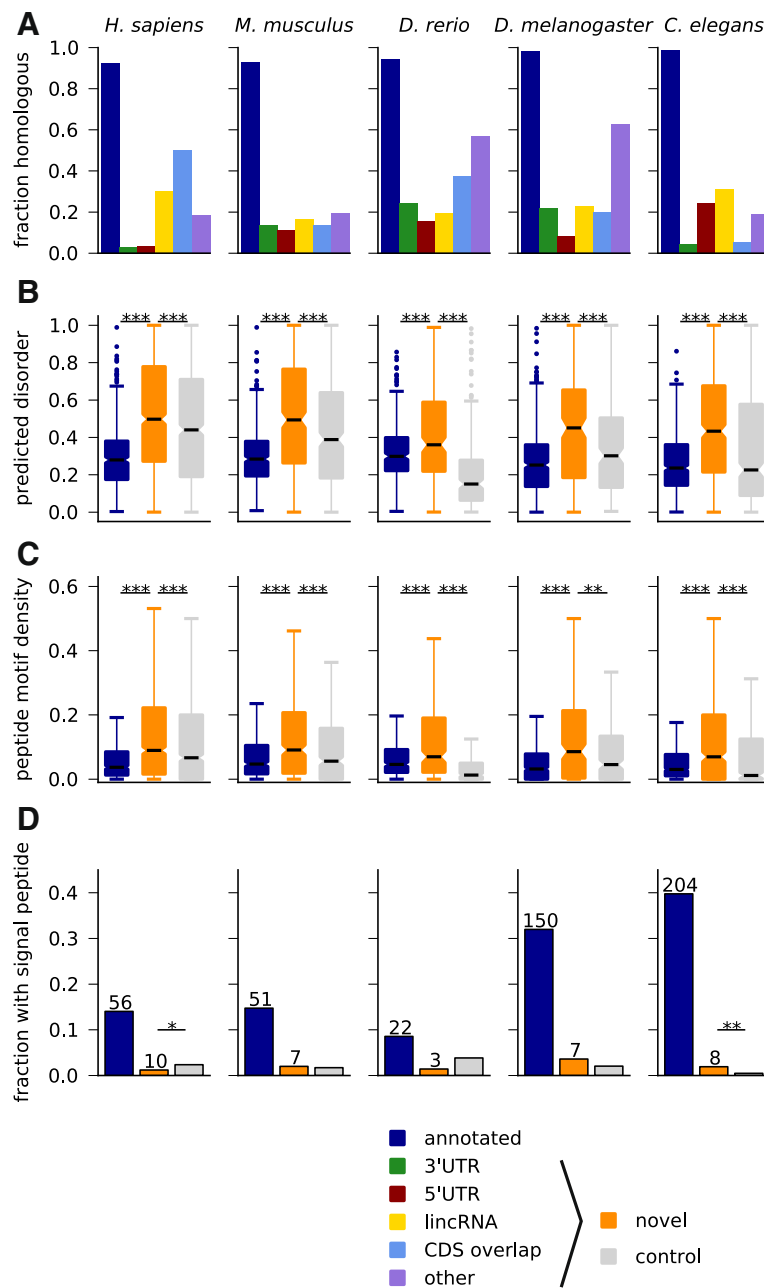


Fig. 4 Properties of encoded peptide sequences. **a** Only a small fraction of novel peptides has significant homology to known longer proteins. **b** Novel predicted peptides are more disordered than annotated short proteins or conceptual products from length-matched control ORFs in non-coding regions, and they also have a higher density of linear peptide motifs (**c**). **d** Some novel sORFs are predicted to contain signal peptide sequences, but not consistently more than expected. *** $P < 0.001$; ** $P < 0.01$; * $P < 0.05$, Mann-Whitney tests in **b** and **c**, binomial test in **d**

file 1: Figure S1C), and they have typically smaller phyloCSF scores (Additional file 7: Figure S2), but nevertheless we were surprised to find so many of them (between 33 in zebrafish and 229 in human). Although the existence of conserved dORFs was observed before [61], and translation was also detected in ribosome profiling [10], to the best of our knowledge there are no known examples of functional peptides produced from 3'UTRs (with the exception of

known polycistronic transcripts). Therefore we explored the possibility that these ORFs actually represent conserved read-through events as suggested previously [35, 71, 72], or come from non-annotated alternative C-terminal exons.

We first checked 283 read-through events in *Drosophila* previously predicted by conservation [71], and 350 detected using ribosome profiling [35]. None of these coincides with any of the 41 sORF candidates

we find in fly 3'UTRs, even though three of the candidates in Jungreis *et al.* [71] were predicted as conserved and only rejected by the overlap filter. Similarly, none of 42 read-through events detected using ribosome profiling in human cells [35] was predicted as conserved. However, three out of eight known or predicted read-through events in human [73] (in MPZ, OPRL1, and OPRK1) and one out of five read-through events predicted in *C. elegans* (in F38E11.6) [71], were here incorrectly classified as 3'UTR sORFs (naturally, they have an in-frame methionine downstream of the annotated stop codon).

Given this small but finite number of false positives, we therefore explored our dORF candidates more systematically. In Fig. 4a, we had already established that dORF-encoded peptides have very little homology to known proteins, in contrast to the domain homology found in *Drosophila* readthrough regions [71]. Next, we checked that there is a very pronounced conservation step near the stop codon of annotated ORFs containing a predicted sORF in their 3'UTR, even though it is slightly smaller than for control ORFs lacking dORFs (Fig. 5a for human; see Additional file 11: Figure S5A for other species). This indicates that sequence downstream of the stop codons is indeed much less conserved and that these stops are not recently acquired (premature) stop codons or unused due to programmed frameshifts upstream. We made a number of further observations arguing against readthrough: dORFs are not generally close to the annotated stop codon or in the same frame, since we find only a small difference in the distribution of these distances and in most cases no preference for a specific reading frame (Fig. 5b and c; Additional file 11: Figure S5B and C); further, we observe a large number

of intervening stop codons (Fig. 5d and Additional file 11: Figure S5D), and a step in conservation near the dORF start codons significantly more pronounced than for control ORFs in 3'UTRs (Fig. 5e and Additional file 11: Figure S5E). In addition, this observation makes it unlikely that dORFs represent non-annotated alternative terminal exons (where this methionine would not be associated with a conservation step). Further, if such unannotated exons existed in large numbers, we would expect that at least some of our (pre-overlap filter) predictions overlap with already annotated alternative exons. However, except for *Drosophila* we only find at most two dORFs with CDS overlap, which is not more than expected compared to non-predicted dORFs (Fig. 5f and Additional file 11: Figure S5F).

In sum, these data suggest that our identification of 3' UTR sORFs is not systematically biased by conserved readthrough events or non-annotated terminal exons. Notably, we also identified candidates that clearly represent independent proteins, such as a 22 aa dORF in the fly gene CG43200 which is likely another one of several ORFs in this polycistronic transcript.

Experimental evidence for translation of and protein expression from predicted sORFs

Finally, we mined a large collection of publicly available and in-house generated data to verify translation of predicted sORFs and associated protein expression. In order to form expectations as to where and how highly our novel candidates could be expressed, we first analyzed publicly available RNA-seq expression datasets for different tissues (human and mouse) or developmental stages (zebrafish, fruit fly, and worm) (Additional file 12: Table S7).

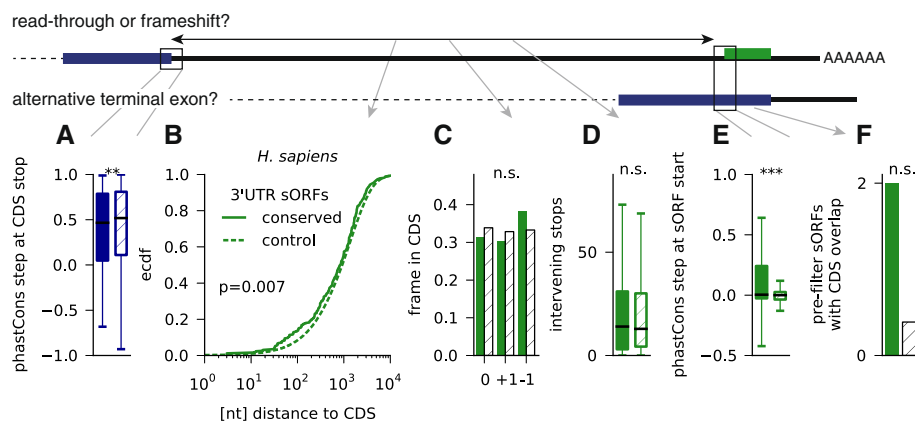


Fig. 5 dORFs (sORFs in 3'UTRs) are not explained by stop-codon read-through or alternative terminal exons. Results are shown for *H. sapiens*. **a** The step in the phastCons conservation track near the stop codon of the upstream CDS is only slightly less pronounced than for CDS without downstream conserved sORF. **b** The dORFs are closer to the CDS than control sORFs, but they are not more often in the same frame (**c**), and they have a similarly high number of intervening in-frame stop codons (**d**). **e** The step in the phastCons conservation track near start of predicted dORFs start is more pronounced than in other dORFs. **f** Even before applying the overlap filter, very few predicted dORFs overlap with annotated coding exons. *** $P < 0.001$; ** $P < 0.01$; * $P < 0.05$; n.s. not significant. Mann-Whitney tests in a, d, and e, Kolmogorov-Smirnov test in b, χ^2 test in c, Binomial test in f

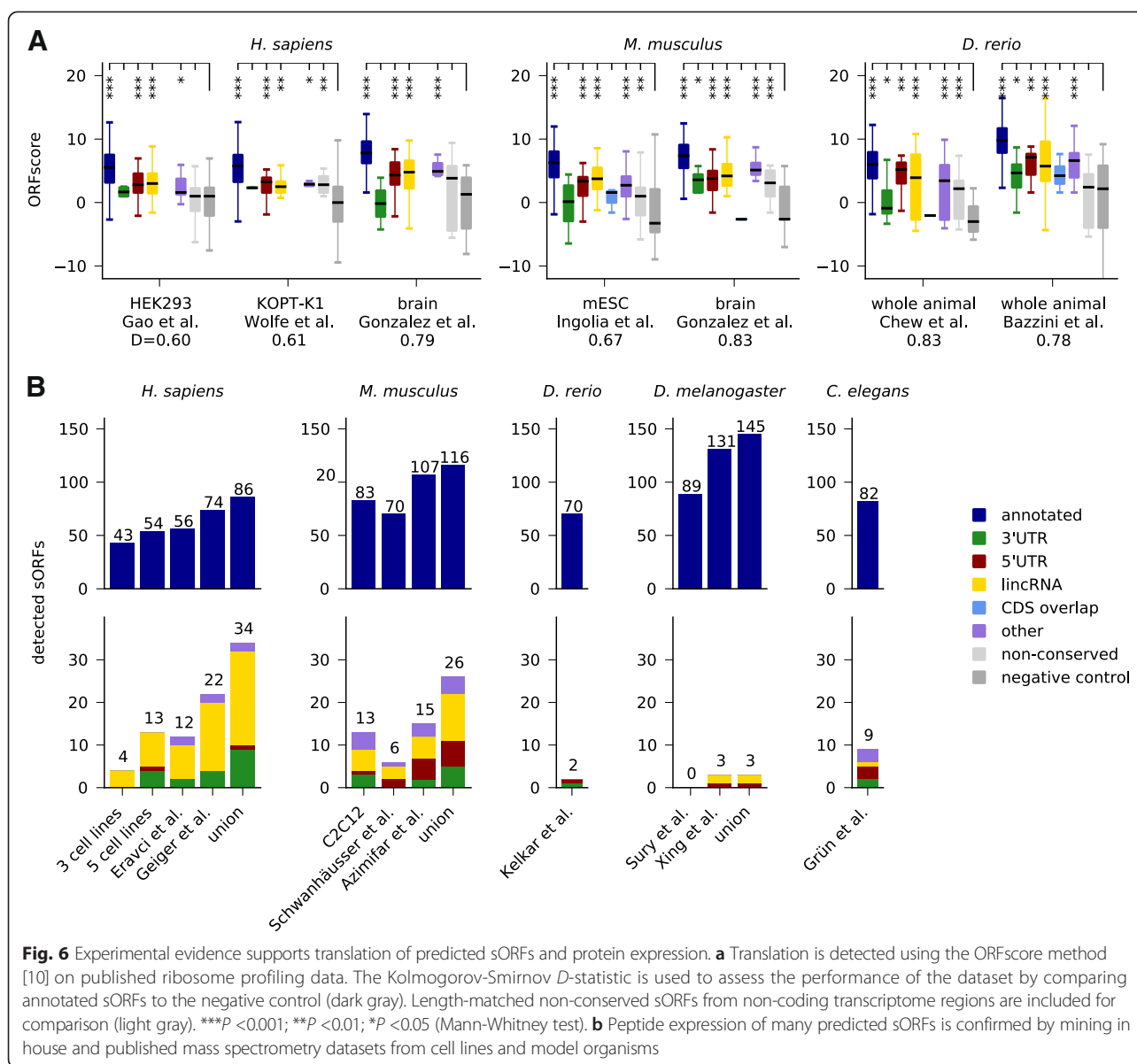
We then compared mRNAs coding for short proteins and lincRNAs with conserved sORFs with other mRNAs and lincRNAs, respectively (Additional file 13: Figure S6A). This analysis revealed that annotated short proteins come from transcripts with higher expression and lower tissue or stage specificity than long proteins. Conversely, we find that lincRNAs with predicted sORFs are more highly and widely expressed than other lincRNAs, but not as highly and widely as protein-coding mRNAs [55, 74]. This analysis indicates that peptide products of novel sORFs could be of lower abundance than known small proteins, and that profiling translation or protein expression from a limited number of cell lines or tissues might not always yield sufficient evidence [11]. We therefore used several datasets for the subsequent analysis.

First, we mined publicly available ribosome profiling datasets in various human and mouse tissues or cell lines, and from zebrafish, fruit fly, and *C. elegans* (Additional file 14: Table S8). Several metrics to identify translated regions from such data have been proposed [9, 14–16]; we rely here on the ORFscore method used in our previous publication [10], which exploits the frame-specific bias of the 5' positions of ribosome protected fragments to distinguish actively translated regions from those transiently associated with ribosomes or contaminants. It requires relatively deep coverage and a very clear 3 nt periodicity in ribosomal fragments, which is not always easily achievable (for example, due to species-specific ribosome conformational properties [11, 35]). We evaluated the ORFscore metric for datasets from human (HEK293 cells [47], KOPT-K1 cells [75] and human brain tissue [76]), mouse (embryonic stem cells [16] and brain tissue [76]), and another zebrafish dataset [9] in addition to the one used before [10]. The performance of these datasets was assessed by comparing ORFscore values of sORFs coding for annotated small proteins to those of the negative control from Fig. 1 by means of the Kolmogorov-Smirnoff D statistic; available datasets for *D. melanogaster* [35] and *C. elegans* [77] did not give a satisfying separation between positive and negative control ($D < 0.55$) and were not used.

Figure 6a shows that predicted lincRNA sORFs have significantly higher ORFscores than the negative control (P values between $8e-7$ and 0.002), and similarly 5'UTR sORFs ($P = 2.5e-7$ to 0.005) and sORFs in the 'other' category ($P = 3.5e-7$ to 0.04). sORFs in 3'UTRs reach marginal significance in some samples ($P = 0.02$ for mouse brain and zebrafish). Choosing an ORFscore cutoff of 6 as done previously [10], we find 45 novel sORFs translated in the human datasets, 15 in mouse, and 50 in zebrafish, respectively. We also find evidence for the translation of some non-conserved sORFs in non-coding regions, indicating that this set could contain lineage-specific or newly evolved coding ORFs or ORFs with regulatory functions.

Next, we searched for peptide evidence in mass spectrometry datasets (Additional file 15: Table S9). We analyzed three in-house datasets to be described in detail elsewhere: one for a mix of three human cell lines (HEK293, HeLa, and K562), one for a mix of five human cell lines (HepG2, MCF-10A, MDA-MB, MCF7, and WI38), and one for murine C2C12 myoblasts and myotubes. Further, we mined several published datasets: one for HEK293 cells [78], one for 11 human cell lines [79], one for mouse NIH3T3 cells [80], one for mouse liver [81], and whole-animal datasets from zebrafish [82], fly [83, 84], and *C. elegans* [85]. All datasets were mapped with MaxQuant [86] against a custom database containing our candidates together with protein sequences from UniProt. PSMs (peptide spectrum matches) were identified at 1% FDR, and those mapping to another sequence in UniProt with one mismatch or ambiguous amino acids were excluded. Using this strategy, we recover between 43 and 131 annotated small proteins per sample and confirm expression for 34 novel predictions in human, 26 in mouse, two in zebrafish, three in fly, and nine in *C. elegans* (Fig. 6b). For instance, we obtain PSMs for the recently described myoregulin micropeptide [31] and for the long isoform of the fly *tarsal-less* gene [26–28]. In total, we find peptidomic evidence for 36 lincRNA sORFs. As observed previously in human [17, 18], mouse [23], and zebrafish [10], we also find PSMs for sORFs in 3'UTRs and 5'UTRs. The MS/MS spectra with peak annotation are shown in Additional file 16: Figure S7, Additional file 17: Figure S8, Additional file 18: Figure S9, Additional file 19: Figure S10, and Additional file 20: Figure S11.

In human and mouse, the results for novel predictions have considerable overlap of 17 and eight hits, respectively, indicating that peptides from some sORFs can be reliably detected in multiple independent experiments. We also find more than one peptide for four and eight novel sORFs in human and mouse and for one sORF in fly and worm, respectively. Likely as a consequence of the differences in expression on the RNA level (Additional file 13: Figure S6A), the PSMs supporting our novel predictions have generally lower intensities than those supporting the positive control (Mann-Whitney $P = 4e-9$; Additional file 13: Figure S6C). However, we also observed that these PSMs have fewer supporting spectra (Additional file 13: Figure S6D), are shorter than those mapping to UniProt proteins ($P = 0.005$; Additional file 13: Figure S6E), and of lower average quality: comparing Andromeda scores and other measures of PSM quality, we found that values for the PSMs supporting expression of novel predictions are smaller than for those mapping to the positive control (Additional file 13: Figure S6F-H). To test for the possibility of misidentifications, we therefore mapped two of our human datasets also against a 3-frame translation of the



entire human transcriptome. As expected given the significantly (7.5-fold) larger database, many PSMs (64 of 240) for annotated and novel sORFs now fall below the 1 % FDR cutoff, but none of the spectra supporting the novel identifications is assigned to a different peptide sequence, and additional PSMs identified in these runs have similarly lower quality. Low-quality identifications can also result when posttranslational modifications of known proteins are not considered during the search [87–89] (Bogdanov *et al.*, under review). We therefore re-mapped one of the human datasets allowing for deamidation or methylation. Both possibilities again lead to a larger search space, such that five and 27 of 117 PSMs, respectively, fail to pass the FDR cutoff. Further,

one of 14 PSMs supporting novel candidates is now attributed to a deamidated protein, but seven of 103 PSMs mapping to sORFs in the positive control are also re-assigned, even though most of these sORFs have independent evidence from other PSMs. Even with our stringent criteria, we found that only about half of the novel sORFs identified in mass spectrometry data have read coverage (>1RPKM) in ribosome profiling data (Additional file 21: Table S10, Additional file 22: Table S11, Additional file 23: Table S12, Additional file 24: Table S13, Additional file 25: Table S14), although the lack of matched samples precludes a rigorous comparison. This uncertainty suggests that targeted mass spectrometry approaches, complementary fragmentation techniques, or

validation runs using synthetic peptides [23] should be used to verify expression of ambiguous candidates.

In summary, we cross-checked our predictions against a variety of high-throughput data: RNA-seq indicates that sORF-harboring lincRNAs are not as highly and widely expressed as other mRNAs, but more than lincRNAs without conserved sORFs. Analyzing ribosome profiling and mass-spectrometry data, we find evidence for translation and protein expression from 110 and 74 novel sORFs, respectively, across all datasets.

Discussion

In our search for functional sORF-encoded peptides, we followed the idea that evolutionary conservation is a strong indicator for functionality if the conservation signal can be reliably separated from background noise and other confounding factors, such as overlapping coding sequences or pseudogenes. We therefore used conservation features that are very specific to known micropeptides (and canonical proteins), namely a depletion of non-synonymous mutations, an absence of frameshifting indels, and characteristic steps in sequence conservation around start and stop codon. We then chose confident sets of positive and negative control sORFs, both of which have many members that are highly conserved on the nucleotide level, and combined these features into a machine learning framework with high sensitivity and specificity. Importantly, our refined pipeline also achieves a more reliable rejection of sORFs on pseudogene transcripts. Pseudogenes are important contaminants since frequent intervening stop codons imply that many of the resulting ORFs are short. While pseudogenes can be translated or under selective constraint [50], sORFs in these genes probably do not represent independent functional or evolutionary units.

Our integrated pipeline identifies sORFs comprehensively and with high accuracy, but we want to highlight a number of caveats and avenues for future research. First, the scope and quality of our predictions depends on the quality of the annotation: in some species, pseudogenes, lincRNAs, and short ncRNAs (especially snoRNAs and snRNAs) have been characterized much more comprehensively, explaining some of the differences in the numbers seen in Fig. 1d. For instance, a recent study suggests that incomplete transcriptome assembly could lead to fragmented lincRNA identifications that obscure the presence of longer ORFs [90]. Second, the performance of our prediction method depends on the choice of the training data: while we aimed to choose negative controls that are transcribed into important RNA species and therefore often conserved on the nucleotide level, the training set is inevitably already separable by length alone, since there are only very few known small peptides below 50 aa, and

very few ORFs on ncRNAs longer than that. A larger number of functionally validated very short ORFs would help to more confidently estimate prediction performance in this length range. In this context, it is important to note that even with low estimated false positive rates we expect a significant number of false discoveries, since the size of the non-coding transcriptome likely far exceeds the amount of true coding sequence. The phyloCSF score can be used to rank candidates by confidence (Additional file 7: Figure S2). Third, we remark that in some cases segmental duplications and/or genomic repeats give rise to a number of redundant sORFs, for instance in a 50 kb region on zebrafish chromosome 9, or on the virtual chromosome U in flies. Fourth, our analysis is currently limited to finding canonical ORFs, even though usage of alternative initiation codons could be widespread [15–17, 46, 47]. Alternative start codon usage might even produce specific conservation signals that could be leveraged to confidently identify ORF boundaries.

Fifth, our approach is limited by the quality of the multiple species alignment: while the micropeptides characterized so far have very clear signatures allowing an alignment-based identification, there could be many instances where sequence conservation within the ORF and its flanking regions is not sufficient to provide robust anchors for a multiple alignment. For instance, functionally homologous micropeptides can be quite diverged on the sequence level. If additional homologous sequence regions can be reliably identified and aligned, a codon-aware re-alignment of candidate sequences [91] could also help to improve detection power. Further, we currently only tested for a depletion of non-synonymous mutations, but more sensitive tests could be implemented in a similar way [51].

Sixth, since we did not find sORFs from our positive control or other known micropeptides to overlap with each other or longer ORFs, we used a quite conservative overlap filter to choose from each genomic locus one ORF most likely to represent an independent evolutionary and functional unit. This filter could be too restrictive: most importantly for sORFs overlapping annotated long ORFs in alternative reading frames, but also when the CDS annotation is incorrect, or for the hypothetical case that a micropeptide has multiple functional splice isoforms.

Finally, we specifically examined 3'UTR sORFs, which are predicted with lower confidence and for which mechanisms of translation are unclear. A very small number of cases could be explained by read-through or alternative exons, but we did not observe global biases. Depending on the experimental conditions, 3'UTR ribosome occupancy can be observed in *Drosophila* and human cells, but it has not been linked to active translation [36]. However,

some mechanisms for downstream initiation have been proposed [92, 93], 3'UTRs can be expressed as distinct RNAs [94], ribosome profiling gives evidence for dORF translation in zebrafish [10], and some peptide products are found by mass-spectrometry [17–19, 22, 23]. Of course, the distinction between uORFs, main CDS, and dORFs becomes blurry for polycistronic transcripts.

To assess putative functionality of the encoded peptides, we tested our candidates for signatures of purifying selection; in addition to the expected depletion of non-synonymous mutations in the multiple alignment when comparing to conservation-matched controls, we also found a weaker (but in many cases highly significant) depletion of non-synonymous SNPs. A closer look at conservation statistics of identified sORFs revealed that many novel predictions are widely conserved between species (for example, almost 350 in placental mammals and almost 40 in jawed vertebrates). By means of sequence similarity clustering, we observed that some of these novel predictions are actually non-annotated homologs of known proteins, but we also found a sizable number of widely conserved uORFs and dORFs. Based on sequence similarity, we could identify six novel predictions that are conserved between vertebrates and invertebrates. This small number is to be expected, since only two of 105 known annotated small proteins similarly conserved are shorter than 50 aa (OST4, a subunit of the oligosaccharyltransferase complex, and ribosomal protein L41), and only a minority of our predicted sORFs is longer than that (about 40 % for zebrafish and 20 % for the other species). Given the recently discovered functional and structural similarities between different SERCA-interacting micropeptides [31, 32], we expect that additional deep homologies between novel micropeptides might emerge in the future.

We also performed a systematic comparison to 16 previously published catalogs of sORF identifications, both computational and by means of high-throughput experiments. While underlying hypotheses, methods, and search criteria varied between studies, they shared the goal of extending genome annotations by identifying novel protein-coding regions. After matching results of other studies to our set of analyzed ORFs, we found in most cases quite limited overlap (Additional file 9: Figure S3), indicating that a broad consensus about sORF characteristics has yet to emerge [37]. However, we observed consistently better indicators of purifying selection for the set of sORFs identified here but not previously versus sORFs identified elsewhere but rejected here. This suggests that our filters result in a high-stringency set of putatively functional sORFs. Of course, even non-conserved sORFs can be functional. Specifically, there could be a continuum between ORFs coding for micropeptides and those with regulatory functions (for example, uORFs): we

previously observed [95] that several uORFs in *Drosophila* with regulatory functions controlled by dedicated re-initiation factors [93] are also predicted here to encode putatively functional peptides, including the fly homolog of the uORF on the vertebrate gene FAM13B. A similar dual role could be fulfilled by sORFs on lincRNAs, whose translation could have the main or additional function of degrading the host transcript via nonsense-mediated decay [12]. Alternatively, such sORFs could represent evolutionary intermediates of novel proteins [62, 65].

To assess transcription, translation, and protein expression of our predicted candidates, we mined high-throughput RNA-seq, ribosome profiling and proteomics datasets. First, we used RNA-seq data to show that sORF-harboring lincRNAs are less highly and widely expressed than mRNAs (this is even more the case for lincRNAs without sORFs). In contrast, mRNAs with annotated sORFs are well and widely expressed, and in fact probably often encode house-keeping genes. Unfortunately, RNA expression is less useful as an expression proxy for the non-lincRNA categories due to an unknown translational coupling between main ORF and uORFs or dORFs. Given these findings, we expect that experiments for many different tissues, developmental time points, and environmental perturbations, and with very deep coverage, would be necessary to exhaustively profile sORF translation and expression. With currently available data, we could confirm translation of more than 100 conserved sORFs in several vertebrate ribosome profiling datasets using a stringent metric (ORFscore [10]), which exploits that actively translated regions lead to a pronounced 3 nt periodicity in the 5' ends of ribosome protected fragments. We also analyzed a number of published and in-house mass spectrometry datasets, and found peptidomic evidence for more than 70 novel candidates.

Many predicted sORF candidates are not detected in the experimental data analyzed here, likely as a consequence of their lower and more restricted expression patterns, which is also one reason for the relatively limited overlap observed when comparing to other experimental studies. Another reason is that experimental and computational methods test different hypotheses. For instance, ribosome profiling provides a comprehensive snapshot of translated regions in the specific cell type, tissue, and/or developmental stage analyzed. This includes sORFs that are translated for regulatory purposes or coding for fast-evolving or lineage-specific peptides such as the small proteins with negative phyloCSF scores excluded from our positive control set. A similar caveat applies to mass-spectrometry, which provides a more direct test of protein expression but has often lower sensitivity than sequencing-based approaches [10, 11], especially for low-molecular-weight peptides. The matching of measured spectra to peptide

sequences is also nontrivial. Especially in deep datasets, low-quality PSMs can result from mismatched database hits if the database is incomplete or frequent post-translational modifications have not been considered [87–89] (Bogdanov *et al.*, under review). It is therefore recommended to combine data from multiple sources when selecting candidates for future studies.

Conclusions

We present an extensively annotated catalog of conserved sORFs in the transcriptomes of five animal species. In addition to recovering known small proteins and recently described micropeptides, we discovered many novel sORFs in non-coding transcriptome regions. Most of these novel candidates show robust and confident signatures of purifying selection and are very short, and some are even widely conserved between species. The encoded micropeptides tend to be disordered and rich in protein interaction motifs. We mined multiple experimental datasets and obtained evidence for translation and protein expression of about 100 and 70 of our candidates, respectively, while RNA expression data suggest that many other novel sORFs will escape detection due to their restricted expression. In summary, combining evolutionary with experimental evidence, our findings provide a confident starting point for functional analyses *in vivo*.

Materials and methods

Transcriptome annotation and alignments

For all species, we used the transcript annotation from Ensembl (v74). Additionally, we used published lincRNA catalogs for human [55, 96], mouse [97], zebrafish [38, 98], and fruit fly [99], and added modENCODE [56] transcripts for *C. elegans*.

We downloaded whole genome multiple species alignments from the UCSC genome browser (human: alignment of 45 vertebrates to hg19, October 2009; mouse: alignment of 59 vertebrates to mm10, April 2014; zebrafish: alignment of seven vertebrates to dr7, May 2011; fruit fly: alignment of 14 insect species to dm3, December 2006; worm: alignment of five nematodes to ce6, June 2008).

ORF definition and classification

Spliced sequences for each transcript were scanned for the longest ORF starting with AUG and with a minimum length of at least 27 nucleotides. We scanned 4,269 unstranded lincRNA transcripts from Young *et al.* [99] on both strands. ORFs from different transcripts but with identical genomic coordinates and amino acid sequence were combined in groups and classified into different categories (using the first matching category for each group): ‘annotated’ if an ORF was identical to the annotated coding sequence of

a protein-coding transcript (that is, biotype ‘protein coding’, and a coding sequence starting at the most upstream AUG, without selenocysteins, read-through, or frameshift events). We classified ORFs as ‘pseudogene’ if a member of a group came from a transcript or a gene locus annotated as pseudogene. We designated as ‘ncRNA’ ORFs (negative controls) those with biotypes miRNA, rRNA, tRNA, snRNA, or snoRNA. Next, ‘3’UTR’ ORFs were classified as such if they resided within the 3’UTRs of canonical protein-coding transcripts, and if they did not overlap with annotated CDS (see below). Analogously, we assigned ‘5’UTR’ ORFs. In the category ‘CDS overlap’ we first collected ORFs that partially overlapped with 3’UTR or 5’UTR of canonical coding transcripts. ORFs in the ‘other’ category were the remaining ones with gene biotype ‘protein coding’, or non-coding RNAs with biotypes ‘sense overlapping’, ‘nonsense-mediated decay’, ‘retained intron’, or other types except ‘lincRNA’. Only those non-coding RNAs with gene and transcript biotype ‘lincRNA’ were designated ‘lincRNA’. To exclude the possibility that alternative reading frames could be translated on transcripts lacking the annotated CDS, we finally added those ORFs that were completely contained in the annotated CDS of canonical transcripts to the ‘CDS overlap’ category if other group members did not fall into the ‘other’ category. Transcripts not from Ensembl were generally designated lincRNAs, except for *C. elegans*: in this case, we merged the modENCODE CDS annotation with Ensembl, and classified only the ‘RIT’ transcripts as non-coding, while the ones that did not match the Ensembl CDS annotation were put in the ‘other’ category. We then added Swiss-Prot and TrEMBL identifiers from the UniProt database (18 November 2014) to our ORFs by matching protein sequences.

Predicting conserved sORFs using a SVM

From the multiple alignments for each ORF, we extracted the species with at least 50 % sequence coverage and without frameshifting indels (using an insertion index prepared before stitching alignment blocks), recording their number as one feature. Stitched alignments for each putative sORF were then scored with PhyloCSF [51] in the omega mode (options `-strategy=omega -f6 -allScores`) and the phylogenetic trees available at UCSC as additional input, yielding a second feature. Finally, we extracted phastCons conservation scores [100] in 50 nt windows around start and stop codon (excluding introns but extending into flanking genomic sequence if necessary) and used the Euclidean distance of the phastCons profiles from the base-wise average over the positive set as third and fourth feature.

A linear support vector machine (LinearSVC implementation in the sklearn package in Python) was built using the four (whitened) conservation features and trained on

positive and negative sets of sORFs. The positive set consisted of those sORFs in the 'annotated' category with encoded peptide sequence listed in Swiss-Prot, with at most 100 aa (101 codons) length, some alignment coverage, and with positive phyloCSF score. The negative set consisted of sORFs from the 'ncRNA' category with alignment coverage, but without overlap with annotated CDS.

We estimated the performance of the classifier by 100 re-sampling runs, where we chose training data from positive and negative set with 50 % probability and predicted on the rest. Prediction of pseudogene sORFs (inset of Fig. 1b) was done either with the SVM, or based on the phyloCSF score alone, using a cutoff of 10 estimated from the minimum average error point in the ROC curve.

Overlap filter

Refining our previous approach [10], we designed an overlap filter as follows: in the first step, we only kept annotated sORFs or those that did not intersect with conserved coding exons. Here we took among the annotated coding exons in Ensembl (v74) or RefSeq (2 September 2014 for mouse, 11 April 2014 for the other species) only those with conserved reading frame, requiring that the number of species without frameshifting indels reaches a threshold chosen from the minimum average error point in the ROC curves of Fig. 1b and Additional file 1: Figure S1 (11 species for human, 10 for mouse, four for zebrafish, seven for fruit fly, and two for worm). In a second step we also required that the remaining ORFs were not contained in a longer ORF (choosing the longest one with the best phyloCSF score) that itself was predicted by the SVM and did not overlap with conserved coding exons.

To exclude CDS overlap for the definition of 3'UTR and 5'UTR sORFs and the design of additional negative controls, we used Ensembl transcripts together with RefSeq (6 February 2014), and added FlyBase (12 December 2013) or modENCODE transcripts [56] for fruit fly and worm, respectively (using intersectBed and a minimum overlap of 1 bp between the ORF and CDS).

Conservation analysis

For the analysis in Figs. 2a and 3, we computed adjusted phyloCSF scores as z-scores over the set of ORFs in the same percentile of the length distribution. Control ORFs were chosen among the non-annotated ORFs without CDS overlap and with their phyloCSF scores chosen among the 20 % closest to zero and then sampled to obtain a statistically indistinguishable distribution of averaged phastCons profiles over the ORF.

SNPs were downloaded as gvf files from Ensembl (for human: v75, 1000 Genomes phase 1; for mouse, zebrafish, and fly: v77); for *C. elegans* we took a list of polymorphisms between the Bristol and Hawaii strains from Vergara et al. [101] and used liftOver to convert ce9

coordinates to ce6. We removed SNPs on the minus strand, SNPs falling into genomic repeats (using the RepeatMasker track from the UCSC genome browser, March 2015), and (if applicable) rare SNPs with derived allele frequency <1 %. We then recorded for each ORF and its conceptual translation the number of synonymous and non-synonymous SNPs, and the number of synonymous and non-synonymous sites. For a set of sORFs, we aggregated these numbers and calculated the dN/dS ratio, where dN is the number of non-synonymous SNPs per non-synonymous site, and dS the number of synonymous SNPs per synonymous site, respectively. The control was chosen as before but without matching for nucleotide level conservation.

Alignment conservation in Fig. 2c was scored by analyzing for each ORF the multiple alignment with respect to the species where start and stop codons and (if applicable) splice sites were conserved, and where premature stop codons or frameshifting indels were absent. We then inferred the common ancestors of these species and plotted the fraction of ORFs with common ancestors at a certain distance to the reference species.

For the graph in Fig. 2d we blasted sORF amino acid sequences from the different reference species against themselves and each other (blastp with options '-evalue 200000 -matrix PAM30 -word_size=2'). We first constructed a directed graph by including hits between sORFs of similar size (at most 20 % deviation) for E-value <10 and an effective percent identity PID_{eff} greater than a dynamically adjusted cutoff that required more sequence identity between shorter matches than longer ones ($PID_{\text{eff}} = (\text{percent identity}) \times (\text{alignment length}) / (\text{query length})$); after inspecting paralogs or orthologs of known candidates such as *tarsal-less* and *toddler* we used the criterion $PID_{\text{eff}} > 30 + 70 \exp(-(\text{query length} + \text{subject length})/20)$. We then removed non-reciprocal edges, and constructed an undirected graph by first obtaining paralog clusters within species (connected components in the single-species subgraphs) and then adding edges for different reference species only for reciprocal best hits between paralog clusters. Finally, we removed singletons. For Fig. 2d, we combined isomorphic subgraphs (regarding sORFs in the same species and of the same type as equivalent), recorded their multiplicity, and plotted only the ones that contain sORFs from at least two different reference species and at least one novel prediction. We then analyzed synteny between vertebrate sORFs in these clusters by using liftOver to convert their genomic coordinates between species, and scored a cluster as syntenic if at least one edge was confirmed by synteny (allowing for a coordinate mismatch of 10 kb to account for splicing changes).

For Additional file 1: Figure S1A we downloaded phastCons conserved elements from the UCSC genome browser (using vertebrate conserved elements for human,

mouse, and zebrafish; 11 November 2014 for human and 27 November 2014 for the other species) and intersected with our set of ORFs; partial overlap means more than 50 % but less than 99 % on the nucleotide level.

Comparison to other studies

We obtained results from other studies in different formats (Additional file 8: Table S6). Tryptic peptide sequences were mapped against the set of ORFs we analyzed (requiring preceding lysine or arginine). Amino acid sequences were directly matched to our set of ORFs, and ORF coordinates were matched to our coordinates (in some cases after conversion between genome versions or the removal of duplicate entries). Since different studies used different annotations and different length cutoffs, we then excluded from the matched ORFs the ones not in the category under consideration, for example, longer ORFs, or sORFs that have since then been annotated or with host transcripts classified as pseudogenes. The remaining ones were compared to our set of predictions.

Sequence analysis of encoded peptides

For Fig. 4a, we used blastp against the RefSeq database (December 2013) and collected among the hits with E-value $>10^{-5}$, percent identity >50 , and query coverage >80 % the best hit (based on percent identity) to entries of the same or larger length that were not flagged as 'PREDICTED', 'hypothetical', 'unknown', 'uncharacterized', or 'putative'.

For the disorder prediction in Fig. 4b, we used IUPred [66] in the 'short' disorder mode and averaged disorder values over the sequence. For the motif discovery in Fig. 4c, we downloaded the file 'elm_classes.tsv' from the ELM database website ([102]; 27 January 2015). We then searched translated ORF sequences for sequence matches to any of the peptide motifs and kept those that fell into regions with average disorder >0.5 . For the signal peptide prediction in Fig. 4d, we used signalp v. 4.1 [70]. Controls in Fig. 4b-d were chosen as in Fig. 2 but matched to the length distribution of novel predicted sORFs.

For Additional file 10: Figure S4A, we counted amino acid usage (excluding start and stop) for all ORFs; amino acids were sorted by their frequency in the positive control ('long ORFs'), which consists of annotated protein-coding ORFs from Swiss-Prot, whereas the negative control is the same as in Figs. 2 and 4 (not matched for conservation or length). We used hierarchical clustering with the correlation metric and average linkage on the frequency distribution for each group, and checked how often we obtained the same two clusters in 100 re-sampling runs where we took a random sample of ORFs in each group with 50 % probability. For Additional file 10: Figure S4B, we counted codon usage, normalized by the amino acid usage, and then calculated a measure of

codon bias for each amino acid using the Kullback-Leibler divergence between the observed distribution of codons per amino acid and a uniform one (in bits). We then performed clustering and bootstrapping as before.

Analysis of 3'UTR sORFs

For all sORFs in the 3'UTR we obtained the annotated CDS of the respective transcript. We then computed the step in the phastCons conservation score (average over 25 nt inside minus average over 25 nt outside) at the stop codon of the annotated CDS and compared protein-coding transcripts with dORFs that are predicted and pass the overlap filter against other protein-coding transcripts. Similarly, we compared the step around the start codons of dORFs. We also compared the distance between the annotated stop and the start of the dORF, the distribution of the reading frame of the dORF start with respect to the annotated CDS, and the number of intervening stops in the frame of the annotated CDS. We finally checked how many predicted dORFs before applying the overlap filter overlap with annotated coding sequence and compared against the remaining dORFs.

We obtained read-through candidates from Supplementary Data 1 in Jungreis *et al.* [71] and from Supplementary Tables 2 and 4 in Dunn *et al.* [35] and matched the corresponding stop codons to stop codons in our set of 3'UTR sORFs.

Expression analysis

For the expression analysis of sORF-containing transcripts we used RNA-seq data for 16 human tissues (Illumina Body Map), for 19 mouse tissues [103], for eight developmental stages of zebrafish [98], 24 developmental stages for fruit fly from modENCODE, and eight developmental stages in *C. elegans* [85] as shown in Additional file 12: Table S7. Reads were mapped to the reference genome using bowtie2 (with options `-very-sensitive`) except for human where we downloaded bam files from Ensembl; replicates were merged and then quantified using cufflinks and the Ensembl (v74) transcript annotation file together with the corresponding lincRNA catalogs. We ignored transcripts with all FPKM values below 10^{-4} and converted to TPM (transcripts per million [104]) as $TPM = 10^6 \text{ FPKM} / (\text{sum of all FPKM})$. Mean expression values were calculated by directly averaging TPM values of transcripts with non-zero TPM values over samples. Tissue or stage specificity was calculated as information content (IC) over the normalized distribution of relative log-transformed expression values $r_t = \frac{\log_2(TPM_t + 1)}{\sum_s \log_2(TPM_s + 1)}$ across tissues or

stages, respectively, using the formula $IC = \frac{1}{\log_2 N} \sum_t r_t \log_2 r_t N$, where N is the number of tissues or stages.

Analysis of published ribosome profiling data

We obtained published ribosome profiling data as summarized in Additional file 14: Table S8. Sequencing reads were stripped from the adapter sequences with the Fastq toolkit. The trimmed reads aligning to rRNA sequences were filtered out using bowtie. The remaining reads were aligned to the genome using STAR, allowing a maximum of five mismatches and ignoring reads that mapped to more than 10 different genomic locations. To reduce the effects of multi-mapping, alignments flagged as secondary alignments were filtered out. We then analyzed read phasing by aggregating 5' read ends over 100 nt windows around start and stop of annotated coding sequences from Ensembl to assess dataset quality and obtain read lengths and 5' offsets for use in scoring. From the datasets in Additional file 14: Table S8 we calculated the ORFscore as described previously [10], pooling the reads from all samples if possible.

Analysis of in-house and published mass spectrometry datasets

We used three in-house generated mass spectrometry datasets that will be described in detail elsewhere: one in a mixture of HEK293, HeLa, and K562 cells, one in a mixture of HepG2, MCF-10A, MDA-DB, MCF7, and WI38 cells, and one in mouse C2C12 myoblasts and myotubes. Further, we mined published datasets using HEK293 cells from Eravci *et al.* [78], using 11 human cell lines from Geiger *et al.* [79], using mouse NIH3T3 cells from Schwanhäusser *et al.* [80], using mouse liver from Azimifar *et al.* [81], using zebrafish whole animals from Kelkar *et al.* [82], using flies from Sury *et al.* [84] and Xing *et al.* [83], and using *C. elegans* from Grün *et al.* [85]. All datasets (Additional file 15: Table S9) were searched individually with MaxQuant v1.4.1.2 [86] against a database containing the entire UniProt reference for that species (Swiss-Prot and TrEMBL; 18 November 2014) merged with a database of common contaminant proteins and the set of predicted (annotated and novel) sORFs (after overlap filter). For fly datasets, an additional *E. coli* database was used. MaxQuant's proteinFDR filter was disabled, while the peptide FDR remained at 1 %. All other parameters were left at default values. To be conservative, we then remapped the identified peptide sequences against the combined database (treating Leucin and Isoleucin as identical and allowing for up to four ambiguous amino acids and one mismatch) with OpenMS [105] and used only those peptides that uniquely mapped to our predictions. Features of PSMs (length, intensity, number of spectra, Andromeda score, intensity coverage, and peak coverage) were extracted from MaxQuant's msms.txt files. When re-mapping two human datasets (HEK293 [78] and five cell lines) against the 3-frame translation of the transcriptome,

we created a custom database from all sequences longer than 7 aa between successive stop codons on transcripts from Ensembl v74 or published lincRNAs [55, 96]. For the re-analysis of the HEK293 dataset [78], we allowed deamidation (NQ) and methylation/methylester (KRCHKNQRIL) as additional variable modifications [88].

Availability of supporting data

Accession codes for the RNA-seq, ribosome profiling and mass spectrometry datasets re-analyzed in this study are listed in Additional file 12: Tables S7, Additional file 14: Table S8, and Additional file 15: Table S9, respectively. The in-house generated mass spectrometry proteomics data have been deposited to the ProteomeXchange Consortium via the PRIDE partner repository with the dataset identifiers PXD002400, PXD002383, and PXD002583.

Additional files

Additional file 1: Figure S1. Overview of the pipeline (relating to Fig. 1). **A** Many sORFs from the positive control and from the negative control overlap fully or partially with phastCons conserved elements. **B** The four conservation features all permit to separate positive from negative control (bottom panels); however, the phyloCSF score contributes most strongly to the SVM classifier. **C** Fraction of sORFs predicted as conserved (pre-overlap filter) for each category. **D** Fraction of sORFs retained after overlap filter in each category. **E** Number of exons spanned by sORFs in different length ranges. (PDF 1063 kb)

Additional file 2: Table S1. All sORF information for human. (TXT 6997 kb)

Additional file 3: Table S2. All sORF information for mouse. (TXT 3192 kb)

Additional file 4: Table S3. All sORF information for zebrafish. (TXT 734 kb)

Additional file 5: Table S4. All sORF information for fly. (TXT 535 kb)

Additional file 6: Table S5. All sORF information for worm. (TXT 1536 kb)

Additional file 7: Figure S2. (Relating to Fig. 2) non-adjusted phyloCSF scores for sORFs in different categories. (PDF 27 kb)

Additional file 8: Table S6. Summary of datasets used in Fig. 3 (other sORF predictions). (ODS 13 kb)

Additional file 9: Figure S3. Comparison between previous studies (relating to Fig. 3) by Venn diagrams for sORFs in the human transcriptome (**A**), in human lincRNAs (**B**), in the mouse transcriptome (**C**), and zebrafish lincRNAs (**D**). Results from this study are used before overlap filter. (PDF 999 kb)

Additional file 10: Figure S4. Sequence features of novel peptides (relating to Fig. 4). **A** Amino acid frequencies in long annotated ORFs, ORFs from non-coding control regions, predicted annotated sORFs and novel predicted sORFs are compared (shown for *H. sapiens*), and a hierarchical clustering is performed. Percentage values indicate how often the same clusters are obtained in a re-sampling analysis. Hydrophobic, acidic, basic, and hydroxyl residues are colored red, blue, magenta, and green, respectively. **B** Codon bias is evaluated from the Kullback-Leibler divergence (Materials and methods). Clustering done as in A. (PDF 911 kb)

Additional file 11: Figure S5. Properties of 3'UTR sORFs (same as Fig. 5 for the other species). (PDF 1026 kb)

Additional file 12: Table S7. Summary of datasets used in Additional file 13: Figure S6A and B (RNA-seq). (ODS 11 kb)

Additional file 13: Figure S6. Expression analysis (relating to Fig. 6). **A** Violin and box plots of mean TPM values for mRNAs hosting predicted annotated sORFs, other mRNAs, lincRNAs hosting predicted novel sORFs, and other lincRNAs, for 16 and 19 tissues in human and mouse, and

eight, 24, and eight developmental stages in zebrafish, fruit fly, and *C. elegans*, respectively. **B** Violin and box plots of tissue or stage specificity for these transcripts. **C** Intensity for PSMs supporting annotated sORFs and peptides supporting novel predicted sORFs, aggregated over all datasets after log-transformation and normalization (z-score) relative to PSMs mapping to UniProt proteins. **D** Number of spectra, **(E)** PSM length, **(F)** Andromeda score, **(G)** peak intensity coverage, and **(H)** peak coverage for the PSMs shown in C. *** $P < 0.001$; ** $P < 0.01$; * $P < 0.05$ (Mann-Whitney tests). (PDF 1042 kb)

Additional file 14: Table S8. Summary of datasets used in Fig. 6a (ribosome profiling). (ODS 14 kb)

Additional file 15: Table S9. Summary of datasets used in Fig. 6b (mass spectrometry). (ODS 13 kb)

Additional file 16: Figure S7. Spectra for the PMS from the human datasets. (PDF 1496 kb)

Additional file 17: Figure S8. Spectra for the PMS from the mouse datasets. (PDF 3586 kb)

Additional file 18: Figure S9. Spectra for the PMS from the zebrafish datasets. (PDF 19 kb)

Additional file 19: Figure S10. Spectra for the PMS from the fly datasets. (PDF 70 kb)

Additional file 20: Figure S11. Spectra for the PMS from the worm datasets. (PDF 65 kb)

Additional file 21: Table S10. Experimental evidence for human sORFs. (ODS 85 kb)

Additional file 22: Table S11. Experimental evidence for mouse sORFs. (ODS 91 kb)

Additional file 23: Table S12. Experimental evidence for zebrafish sORFs. (ODS 49 kb)

Additional file 24: Table S13. Experimental evidence for fruit fly sORFs. (ODS 69 kb)

Additional file 25: Table S14. Experimental evidence for *C. elegans* sORFs. (ODS 43 kb)

Competing interests

The authors declare that they have no competing interests.

Authors' contributions

NR and SDM initiated the project. SDM and BO designed and performed research for this paper. DT and BO performed conservation, sequence, and expression analyses. SDM, LC, and BO analyzed ribosome profiling data. HZ, CB, KK, GM, and BO analyzed mass spectrometry data, supervised by SK and MS. BO prepared figures and wrote the paper, with input from the other authors. All authors read and approved the final manuscript.

Acknowledgements

We thank the Nikolaus Rajewsky lab for fruitful discussion, and Fabian Bindel for sharing unpublished mass-spec datasets. SDM and NR thank Francois Payre for initial discussions. KK is funded by the MDC/NYU exchange program, LC by the MDC international PhD program, and BO gratefully acknowledges a Max-Delbrück fellowship of the MDC.

Author details

¹Berlin Institute for Medical Systems Biology, Max-Delbrück-Center for Molecular Medicine, Robert-Rössle-Str. 10, 13125 Berlin, Germany. ²Berlin Institute of Health, Kapelle-Ufer 2, 10117 Berlin, Germany.

Received: 23 April 2015 Accepted: 5 August 2015

Published online: 14 September 2015

References

1. ENCODE Project Consortium, Birney E, Stamatoyannopoulos JA, Dutta A, Guigo R, Gingeras TR, et al. Identification and analysis of functional elements in 1% of the human genome by the ENCODE pilot project. *Nature*. 2007;447:799–816.

2. Ulitsky I, Bartel DP. lincRNAs: Genomics, evolution, and mechanisms. *Cell*. 2013;154:26–46.
3. Engreitz JM, Pandya-Jones A, McDonel P, Shishkin A, Sirokman K, Surka C, et al. The Xist lincRNA exploits three-dimensional genome architecture to spread across the X chromosome. *Science*. 2013;341:1237973.
4. Cesana M, Cacchiarelli D, Legnini I, Santini T, Sthandier O, Chinappi M, et al. A long noncoding RNA controls muscle differentiation by functioning as a competing endogenous RNA. *Cell*. 2011;147:358–69.
5. Bassett AR, Akhtar A, Barlow DP, Bird AP, Brockdorff N, Duboule D, et al. Considerations when investigating lincRNA function in vivo. *Elife*. 2014;3:e03058.
6. Dinger ME, Pang KC, Mercer TR, Mattick JS. Differentiating protein-coding and noncoding RNA: challenges and ambiguities. *PLoS Comput Biol*. 2008;4:e1000176.
7. van Heesch S, van Iterson M, Jacobi J, Boymans S, Essers PB, de Bruijn E, et al. Extensive localization of long noncoding RNAs to the cytosol and mono- and polyribosomal complexes. *Genome Biol*. 2014;15:R6.
8. Wilson BA, Masel J. Putatively noncoding transcripts show extensive association with ribosomes. *Genome Biol Evol*. 2011;3:1245–52.
9. Chew G-L, Pauli A, Rinn JL, Regev A, Schier AF, Valen E. Ribosome profiling reveals resemblance between long non-coding RNAs and 5' leaders of coding RNAs. *Development*. 2013;140:2828–34.
10. Bazzini AA, Johnstone TG, Christiano R, Mackowiak SD, Obermayer B, Fleming ES, et al. Identification of small ORFs in vertebrates using ribosome footprinting and evolutionary conservation. *Embo J*. 2014;33:981–93.
11. Aspden JL, Eyre-Walker YC, Phillips RJ, Amin U, Mumtaz MAS, Brocard M, et al. Extensive translation of small open reading frames revealed by Poly-Ribo-Seq. *Elife*. 2014;3:e03528.
12. Smith JE, Alvarez-Dominguez JR, Kline N, Huynh NJ, Geisler S, Hu W, et al. Translation of small open reading frames within unannotated RNA transcripts in *Saccharomyces cerevisiae*. *Cell Rep*. 2014;7:1858.
13. Banfai B, Jia H, Khatun J, Wood E, Risk B, Gundling WE, et al. Long noncoding RNAs are rarely translated in two human cell lines. *Genome Res*. 2012;22:1646–57.
14. Guttman M, Russell P, Ingolia NT, Weissman JS, Lander ES. Ribosome profiling provides evidence that large noncoding RNAs do not encode proteins. *Cell*. 2013;154:240–51.
15. Ingolia NT, Brar GA, Stern-Ginossar N, Harris MS, Talhouarne GJS, Jackson SE, et al. Ribosome profiling reveals pervasive translation outside of annotated protein-coding genes. *Cell Rep*. 2014;8:1365.
16. Ingolia NT, Lareau LF, Weissman JS. Ribosome profiling of mouse embryonic stem cells reveals the complexity and dynamics of mammalian proteomes. *Cell*. 2011;147:789–802.
17. Slavoff SA, Mitchell AJ, Schwaid AG, Cabili MN, Ma J, Levin JZ, et al. Peptidomic discovery of short open reading frame–encoded peptides in human cells. *Nat Chem Biol*. 2012;9:59–64.
18. Vanderperre B, Lucier J-F, Bissonnette C, Motard J, Tremblay G, Vanderperre S, et al. Direct detection of alternative open reading frames translation products in human significantly expands the proteome. *PLoS ONE*. 2013;8:e70698.
19. Ma J, Ward CC, Jungreis I, Slavoff SA, Schwaid AG, Neveu J, et al. Discovery of human sORF-encoded polypeptides (SEPs) in cell lines and tissue. *J Proteome Res*. 2014;13:1757–65.
20. Wilhelm M, Schlegl J, Hahne H, Gholami AM, Lieberenz M, Savitski MM, et al. Mass-spectrometry-based draft of the human proteome. *Nature*. 2014;509:582–7.
21. Kim M-S, Pinto SM, Getnet D, Nirujogi RS, Manda SS, Chaerkady R, et al. A draft map of the human proteome. *Nature*. 2014;509:575–81.
22. Gascoigne DK, Cheetham SW, Cattenoz PB, Clark MB, Amaral PP, Taff RJ, et al. PinStripe: a suite of programs for integrating transcriptomic and proteomic datasets identifies novel proteins and improves differentiation of protein-coding and non-coding genes. *Bioinformatics*. 2012;28:3042–50.
23. Prabhakaran S, Hemberg M, Chauhan R, Winter D, Tweedie-Cullen RY, Dittrich C, et al. Quantitative profiling of peptides from RNAs classified as noncoding. *Nat Commun*. 2014;5:5429.
24. Senar ML, Delgado J, Chen WH, Rico VL, O'Reilly FJ, Wodke JA, et al. Defining a minimal cell: essentiality of small ORFs and ncRNAs in a genome-reduced bacterium. *Mol Syst Biol*. 2015;11:780.
25. Kastenmayer JP, Ni L, Chu A, Kitchen LE, Au W-C, Yang H, et al. Functional genomics of genes with small open reading frames (sORFs) in *S. cerevisiae*. *Genome Res*. 2006;16:365–73.

26. Galindo MI, Pueyo JI, Fouix S, Bishop SA, Couso JP. Peptides encoded by short ORFs control development and define a new eukaryotic gene family. *PLoS Biol.* 2007;5:e106.
27. Savard J, Marques-Souza H, Aranda M, Tautz D. A segmentation gene in *tribolium* produces a polycistronic mRNA that codes for multiple conserved peptides. *Cell.* 2006;126:559–69.
28. Kondo T, Hashimoto Y, Kato K, Inagaki S, Hayashi S, Kageyama Y. Small peptide regulators of actin-based cell morphogenesis encoded by a polycistronic mRNA. *Nat Cell Biol.* 2007;9:660–5.
29. Kondo T, Plaza S, Zanet J, Benrabah E, Valenti P, Hashimoto Y, et al. Small peptides switch the transcriptional activity of *Shavenbaby* during *Drosophila* embryogenesis. *Science.* 2010;329:336–9.
30. Pauli A, Norris ML, Valen E, Chew G-L, Gagnon JA, Zimmerman S, et al. Toddler: an embryonic signal that promotes cell movement via Apelin receptors. *Science.* 2014;343:1248636.
31. Anderson DM, Anderson KM, Chang C-L, Makarewich CA, Nelson BR, McAnally JR, et al. A micropeptide encoded by a putative long noncoding RNA regulates muscle performance. *Cell.* 2015;160:595–606.
32. Magny EG, Pueyo JI, Pearl FMG, Cespedes MA, Niven JE, Bishop SA, et al. Conserved regulation of cardiac calcium uptake by peptides encoded in small open reading frames. *Science.* 2013;341:1116–20.
33. Somers J, Pöyry T, Willis AE. A perspective on mammalian upstream open reading frame function. *Int J Biochem Cell Biol.* 2013;45:1690–700.
34. Calvo SE, Pagliarini DJ, Mootha VK. Upstream open reading frames cause widespread reduction of protein expression and are polymorphic among humans. *Proc Natl Acad Sci.* 2009;106:7507–12.
35. Dunn JG, Foo CK, Belletier NG, Gavis ER, Weissman JS, Sonenberg N. Ribosome profiling reveals pervasive and regulated stop codon readthrough in *Drosophila melanogaster*. *Elife.* 2013;2:e01179.
36. Miettinen TP, Björklund M. Modified ribosome profiling reveals high abundance of ribosome protected mRNA fragments derived from 3' untranslated regions. *Nucleic Acids Res.* 2015;43:1019–34.
37. Andrews SJ, Rothnagel JA. Emerging evidence for functional peptides encoded by short open reading frames. *Nat Rev Genet.* 2014;15:193–204.
38. Ulitsky I, Shkumatava A, Jan CH, Sive H, Bartel DP. Conserved Function of lincRNAs in Vertebrate Embryonic Development despite Rapid Sequence Evolution. *Cell.* 2011;147:1537–50.
39. Hezroni H, Koppstein D, Schwartz MG, Avrutin A, Bartel DP, Ulitsky I. Principles of long noncoding RNA evolution derived from direct comparison of transcriptomes in 17 species. *Cell Rep.* 2015;11:1110–22.
40. Kellis M, Patterson N, Birren B, Berger B, Lander ES. Methods in comparative genomics: genome correspondence, gene identification and regulatory motif discovery. *J Comput Biol.* 2004;11:319–55.
41. Kellis M, Patterson N, Endrizzi M, Birren B, Lander ES. Sequencing and comparison of yeast species to identify genes and regulatory elements. *Nature.* 2003;423:241–54.
42. Wang L, Park HJ, Dasari S, Wang S, Kocher J-P, Li W. CPAT: Coding-potential assessment tool using an alignment-free logistic regression model. *Nucleic Acids Res.* 2013;41:e74.
43. Burge CB, Karlin S. Finding the genes in genomic DNA. *Curr Opin Struct Biol.* 1998;8:346–54.
44. Ladoukakis E, Pereira V, Magny EG, Eyre-Walker A, Couso JP. Hundreds of putatively functional small open reading frames in *Drosophila*. *Genome Biol.* 2011;12:R118.
45. Crappé J, Van Criekeing W, Trooskens G, Hayakawa E, Luyten W, Baggerman G, et al. Combining in silico prediction and ribosome profiling in a genome-wide search for novel putatively coding sORFs. *BMC Genomics.* 2013;14:648.
46. Lee S, Liu B, Lee S, Huang S-X, Shen B, Qian S-B. Global mapping of translation initiation sites in mammalian cells at single-nucleotide resolution. *Proc Natl Acad Sci.* 2012;109:E2424–32.
47. Gao X, Wan J, Liu B, Ma M, Shen B, Qian S-B. Quantitative profiling of initiating ribosomes in vivo. *Nat Methods.* 2014;12:147.
48. Marques AC, Tan J, Lee S, Kong L, Heger A, Ponting CP. Evidence for conserved post-transcriptional roles of unitary pseudogenes and for frequent bifunctionality of mRNAs. *Genome Biol.* 2012;13:R102.
49. Pink RC, Wicks K, Caley DP, Punch EK, Jacobs L, Francisco Carter DR. Pseudogenes: Pseudo-functional or key regulators in health and disease? *RNA.* 2011;17:792.
50. Pei B, Sisu C, Frankish A, Howald C, Habegger L, Mu XJ, et al. The GENCODE pseudogene resource. *Genome Biol.* 2012;13:R51.
51. Lin MF, Jungreis I, Kellis M. PhyloCSF: a comparative genomics method to distinguish protein coding and non-coding regions. *Bioinformatics.* 2011;27:i275–82.
52. Rè M, Pesole G, Horner DS. Accurate discrimination of conserved coding and non-coding regions through multiple indicators of evolutionary dynamics. *BMC Bioinformatics.* 2009;10:282.
53. Hanyu-Nakamura K, Sonobe-Nojima H, Tanigawa A, Lasko P, Nakamura A. *Drosophila* Pgc protein inhibits P-TEFb recruitment to chromatin in primordial germ cells. *Nature.* 2008;451:730–3.
54. Escobar B, de Carcer G, Fernandez-Miranda G, Cascon A, Bravo-Cordero JJ, Montoya MC, et al. Brick1 is an essential regulator of actin cytoskeleton required for embryonic development and cell transformation. *Cancer Res.* 2010;70:9349–59.
55. Cabili MN, Trapnell C, Goff L, Koziol M, Tazon-Vega B, Regev A, et al. Integrative annotation of human large intergenic noncoding RNAs reveals global properties and specific subclasses. *Genes Dev.* 2011;25:1915–27.
56. Gerstein MB, Lu ZJ, Van Nostrand EL, Cheng C, Arshinoff BI, Liu T, et al. Integrative analysis of the *Caenorhabditis elegans* genome by the modENCODE Project. *Science.* 2010;330:1775–87.
57. Akimoto C, Sakashita E, Kasashima K, Kuroiwa K, Tominaga K, Hamamoto T, et al. Translational repression of the Mckusick-Kaufman syndrome transcript by unique upstream open reading frames encoding mitochondrial proteins with alternative polyadenylation sites. *Biochim Biophys Acta.* 2013;1830:2728–38.
58. Iuchi S. Three classes of C2H2 zinc finger proteins. *Cell Mol Life Sci.* 2001;58:625–35.
59. Allen RJ, Brenner EP, VanOrsdel CE, Hobson JJ, Hearn DJ, Hemm MR. Conservation analysis of the CydX protein yields insights into small protein identification and evolution. *BMC Genomics.* 2014;15:946.
60. Frith MC, Forrest AR, Nourbakhsh E, Pang KC, Kai C, Kawai J, et al. The abundance of short proteins in the mammalian proteome. *PLoS Genet.* 2006;2:e52.
61. Crowe ML, Wang X-Q, Rothnagel JA. Evidence for conservation and selection of upstream open reading frames suggests probable encoding of bioactive peptides. *BMC Genomics.* 2006;7:16.
62. Ruiz-Orera J, Messeguer X, Subirana JA, Albà MM, Tautz D. Long non-coding RNAs as a source of new peptides. *Elife.* 2014;3:e03523.
63. Vanderperre B, Lucier J-F, Roucou X. HAltORF: a database of predicted out-of-frame alternative open reading frames in human. *Database (Oxford).* 2012;2012:bas025.
64. Chung W-Y, Wadhawan S, Szklarczyk R, Pond SK, Nekrutenko A. A first look at ARFome: dual-coding genes in mammalian genomes. *PLoS Comput Biol.* 2007;3:e91.
65. Carvunis A-R, Rolland T, Wapinski I, Calderwood MA, Yildirim MA, Simonis N, et al. Proto-genes and de novo gene birth. *Nature.* 2012;487:370–4.
66. Dosztányi Z, Csizmok V, Tompa P, Simon I. IUPred: web server for the prediction of intrinsically unstructured regions of proteins based on estimated energy content. *Bioinformatics.* 2005;21:3433–4.
67. Dyson HJ, Wright PE. Intrinsically unstructured proteins and their functions. *Nat Rev Mol Cell Bio.* 2005;6:197–208.
68. Tompa P, Davey NE, Gibson TJ, Babu MM. A million peptide motifs for the molecular biologist. *Mol Cell.* 2014;55:161–9.
69. Dinkel H, Van Roey K, Michael S, Davey NE, Weatheritt RJ, Born D, et al. The eukaryotic linear motif resource ELM: 10 years and counting. *Nucleic Acids Res.* 2014;42:D259–66.
70. Nielsen H, Engelbrecht J, Brunak S, von Heijne G. Identification of prokaryotic and eukaryotic signal peptides and prediction of their cleavage sites. *Protein Eng.* 1997;10:1–6.
71. Jungreis I, Lin MF, Spokony R, Chan CS, Negre N, Victorsen A, et al. Evidence of abundant stop codon readthrough in *Drosophila* and other metazoa. *Genome Res.* 2011;21:2096–113.
72. Lin MF, Carlson JW, Crosby MA, Matthews BB, Yu C, Park S, et al. Revisiting the protein-coding gene catalog of *Drosophila melanogaster* using 12 fly genomes. *Genome Res.* 2007;17:1823–36.
73. Loughran G, Chou MY, Ivanov IP, Jungreis I, Kellis M, Kiran AM, et al. Evidence of efficient stop codon readthrough in four mammalian genes. *Nucleic Acids Res.* 2014;42:8928–38.
74. Guttman M, Amit I, Garber M, French C, Lin MF, Feldser D, et al. Chromatin signature reveals over a thousand highly conserved large non-coding RNAs in mammals. *Nature.* 2009;458:223–7.

75. Wolfe AL, Singh K, Zhong Y, Drewe P, Rajasekhar VK, Sanghvi VR, et al. RNA G-quadruplexes cause eIF4A-dependent oncogene translation in cancer. *Nature*. 2014;513:65–70.
76. Gonzalez C, Sims JS, Hornstein N, Mela A, Garcia F, Lei L, et al. Ribosome profiling reveals a cell-type-specific translational landscape in brain tumors. *J Neurosci*. 2014;34:10924–36.
77. Stadler M, Fire A. Conserved translome remodeling in nematode species executing a shared developmental transition. *PLoS Genet*. 2013;9:e1003739.
78. Eravci M, Sommer C, Selbach M. IPG strip-based peptide fractionation for shotgun proteomics. *Methods Mol Biol*. 2014;1156:67–77.
79. Geiger T, Wehner A, Schaab C, Cox J, Mann M. Comparative proteomic analysis of eleven common cell lines reveals ubiquitous but varying expression of most proteins. *Mol Cell Proteomics*. 2012;11:M111.014050.
80. Schwanhäusser B, Busse D, Li N, Dittmar G, Schuchhardt J, Wolf J, et al. Global quantification of mammalian gene expression control. *Nature*. 2011;473:337–42.
81. Azimifar SB, Nagaraj N, Cox J, Mann M. Cell-type-resolved quantitative proteomics of murine liver. *Cell Metab*. 2014;20:1076–87.
82. Kelkar DS, Provost E, Chaerkady R, Muthusamy B, Manda SS, Subbannayya T, et al. Annotation of the zebrafish genome through an integrated transcriptomic and proteomic analysis. *Mol Cell Proteomics*. 2014;13:3184–98.
83. Xing X, Zhang C, Li N, Zhai L, Zhu Y, Yang X, et al. Qualitative and quantitative analysis of the adult *Drosophila melanogaster* proteome. *Proteomics*. 2014;14:286–90.
84. Sury MD, Chen J-X, Selbach M. The SILAC fly allows for accurate protein quantification in vivo. *Mol Cell Proteomics*. 2010;9:2173–83.
85. Grün D, Kirchner M, Thierfelder N, Stoeckius M, Selbach M, Rajewsky N. Conservation of mRNA and protein expression during development of *C. elegans*. *Cell Rep*. 2014;6:565–77.
86. Cox J, Neuhäuser N, Michalski A, Scheltema RA, Olsen JV, Mann M. Andromeda: a peptide search engine integrated into the MaxQuant environment. *J Proteome Res*. 2011;10:1794–805.
87. Nielsen ML, Savitski MM, Zubarev RA. Extent of modifications in human proteome samples and their effect on dynamic range of analysis in shotgun proteomics. *Mol Cell Proteomics*. 2006;5:2384–91.
88. Savitski MM, Nielsen ML, Zubarev RA. ModifiComb, a new proteomic tool for mapping substoichiometric post-translational modifications, finding novel types of modifications, and fingerprinting complex protein mixtures. *Mol Cell Proteomics*. 2006;5:935–48.
89. Chick JM, Kolippakkam D, Nusinow DP, Zhai B, Rad R, Huttlin EL, et al. A mass-tolerant database search identifies a large proportion of unassigned spectra in shotgun proteomics as modified peptides. *Nat Biotechnol*. 2015;33:743.
90. Iyer MK, Niknafs YS, Malik R, Singhal U, Sahu A, Hosono Y, et al. The landscape of long noncoding RNAs in the human transcriptome. *Nat Genet*. 2015;47:199–208.
91. Ranwez V, Harispe S, Delsuc F, Douzery EJP. MACSE: Multiple Alignment of Coding SEquences accounting for frameshifts and stop codons. *PLoS ONE*. 2011;6:e22594.
92. Paek KY, Hong KY, Ryu I, Park SM, Keum SJ, Kwon OS, et al. Translation initiation mediated by RNA looping. *Proc Natl Acad Sci*. 2015;112:1041–6.
93. Schleich S, Strassburger K, Janiesch PC, Koledachkina T, Miller KK, Haneke K, et al. DENR-MCT-1 promotes translation re-initiation downstream of uORFs to control tissue growth. *Nature*. 2014;512:208.
94. Mercer TR, Wilhelm D, Dingler ME, Solda G, Korbie DJ, Glazov EA, et al. Expression of distinct RNAs from 3' untranslated regions. *Nucleic Acids Res*. 2011;39:2393–403.
95. Obermayer B, Rajewsky N. Mixed messages: Re-initiation factors regulate translation of animal mRNAs. *Cell Res*. 2014;24:1383–4.
96. Derrien T, Johnson R, Bussotti G, Tanzer A, Djebali S, Tilgner H, et al. The GENCODE v7 catalog of human long noncoding RNAs: analysis of their gene structure, evolution, and expression. *Genome Res*. 2012;22:1775–89.
97. Guttman M, Garber M, Levin JZ, Donaghey J, Robinson J, Adiconis X, et al. Ab initio reconstruction of cell type-specific transcriptomes in mouse reveals the conserved multi-exonic structure of lincRNAs. *Nat Biotechnol*. 2010;28:503–10.
98. Pauli A, Valen E, Lin MF, Garber M, Vastenhouw NL, Levin JZ, et al. Systematic identification of long noncoding RNAs expressed during zebrafish embryogenesis. *Genome Res*. 2012;22:577–91.
99. Young RS, Marques AC, Tibbit C, Haerty W, Bassett AR, Liu JL, et al. Identification and properties of 1,119 candidate lincRNA loci in the *Drosophila melanogaster* genome. *Genome Biol Evol*. 2012;4:427–42.
100. Siepel A, Bejerano G, Pedersen JS, Hinrichs AS, Hou M, Rosenbloom K, et al. Evolutionarily conserved elements in vertebrate, insect, worm, and yeast genomes. *Genome Res*. 2005;15:1034–50.
101. Vergara IA, Tarailo-Graovac M, Frech C, Wang J, Qin Z, Zhang T, et al. Genome-wide variations in a natural isolate of the nematode *Caenorhabditis elegans*. *BMC Genomics*. 2014;15:255.
102. The Eukaryotic Linear Motif Resource for Functional Sites in Proteins. Available at: <http://elm.eu.org/downloads.html>.
103. Shen Y, Yue F, McCleary DF, Ye Z, Edsall L, Kuan S, et al. A map of the cis-regulatory sequences in the mouse genome. *Nature*. 2012;488:116–20.
104. Wagner GP, Kin K, Lynch VJ. Measurement of mRNA abundance using RNA-seq data: RPKM measure is inconsistent among samples. *Theory Biosci*. 2012;131:281–5.
105. Sturm M, Bertsch A, Gröpl C, Hildebrandt A, Hussong R, Lange E, et al. OpenMS - an open-source software framework for mass spectrometry. *BMC Bioinformatics*. 2008;9:163.

Submit your next manuscript to BioMed Central and take full advantage of:

- Convenient online submission
- Thorough peer review
- No space constraints or color figure charges
- Immediate publication on acceptance
- Inclusion in PubMed, CAS, Scopus and Google Scholar
- Research which is freely available for redistribution

Submit your manuscript at
www.biomedcentral.com/submit

